

Ga-Bivalent Polypegylated Styrylpyridine Conjugates for Imaging A β Plaques in Cerebral Amyloid Angiopathy (CAA)

Zhihao Zha, Jin Song, Seok Rye Choi, Zehui Wu, Karl Ploessl, Megan Smith, and Hank F. Kung

Bioconjugate Chem., **Just Accepted Manuscript** • DOI: 10.1021/acs.bioconjchem.6b00127 • Publication Date (Web): 04 Apr 2016

Downloaded from <http://pubs.acs.org> on April 6, 2016

Just Accepted

“Just Accepted” manuscripts have been peer-reviewed and accepted for publication. They are posted online prior to technical editing, formatting for publication and author proofing. The American Chemical Society provides “Just Accepted” as a free service to the research community to expedite the dissemination of scientific material as soon as possible after acceptance. “Just Accepted” manuscripts appear in full in PDF format accompanied by an HTML abstract. “Just Accepted” manuscripts have been fully peer reviewed, but should not be considered the official version of record. They are accessible to all readers and citable by the Digital Object Identifier (DOI®). “Just Accepted” is an optional service offered to authors. Therefore, the “Just Accepted” Web site may not include all articles that will be published in the journal. After a manuscript is technically edited and formatted, it will be removed from the “Just Accepted” Web site and published as an ASAP article. Note that technical editing may introduce minor changes to the manuscript text and/or graphics which could affect content, and all legal disclaimers and ethical guidelines that apply to the journal pertain. ACS cannot be held responsible for errors or consequences arising from the use of information contained in these “Just Accepted” manuscripts.

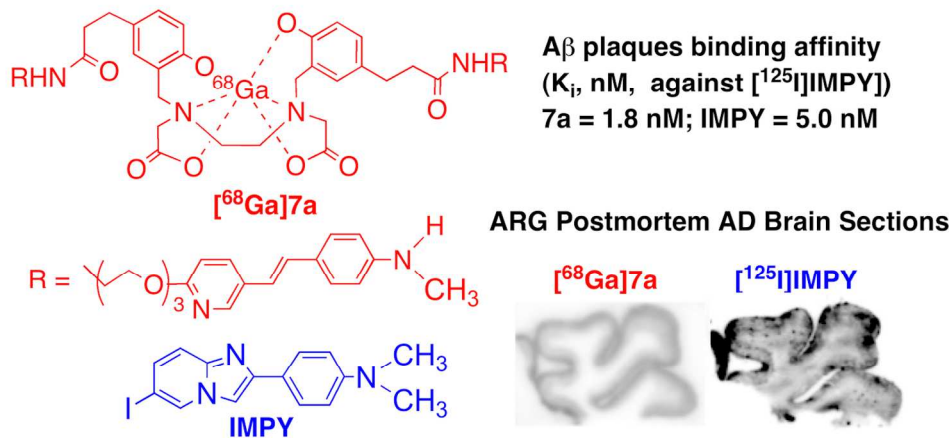
Imaging A β Plaques in Cerebral Amyloid Angiopathy**⁶⁸Ga-Bivalent Polypegylated Styrylpyridine Conjugates for Imaging A β Plaques in Cerebral Amyloid Angiopathy (CAA)**

Zhihao Zha^{a,c}, Jin Song^{a,c}, Seok Rye Choi^{b,c}, Zehui Wu^{a,c}, Karl Ploessl^{b,c}, Megan Smith^b, Hank Kung^{a,b,c*}

^aBeijing Institute for Brain Disorders, Capital Medical University, Beijing, 100069, China; ^bFive Eleven Pharma Inc., Philadelphia, PA 19104; ^cDepartment of Radiology, University of Pennsylvania, Philadelphia, PA 19104, USA

*Corresponding author contact information:

Hank F. Kung, Ph.D. Department of Radiology, University of Pennsylvania, 3700 Market Street, Room 305, Philadelphia, PA 19104, USA Tel: +1 215 662 3989; Fax: +1 215 349 5035; E-mail: kunghf@sunmac.spect.upenn.edu (H.F. Kung)

Imaging A β Plaques in Cerebral Amyloid Angiopathy**Abstract:**

A β plaques deposited on blood vessels are associated with cerebral amyloid angiopathy (CAA). In an effort to selectively map these A β plaques, we are reporting a new series of ^{68}Ga labeled styrylpyridine derivatives with high molecular weights. *In vitro* binding to A β plaques in postmortem Alzheimer's disease (AD) brain tissue showed that these ^{68}Ga labeled bivalent styrylpyridines displayed good affinities and specificity ($K_i < 30 \text{ nM}$). *In vitro* autoradiography using postmortem AD brain sections showed specific binding of these ^{68}Ga complexes to A β plaques. Biodistribution studies in normal mice showed very low initial brain uptakes ($< 0.3\% \text{ dose/g}$) indicating a low blood-brain barrier (BBB) penetration. The preliminary results suggest that ^{68}Ga labeled bivalent styrylpyridines may be promising candidates as PET imaging radiotracers for detecting CAA.

Key Words: cerebral amyloid angiopathy, A β plaques, Alzheimer's disease, positron emission tomography, molecular imaging, autoradiography and biodistribution.

Imaging A β Plaques in Cerebral Amyloid Angiopathy**Introduction:**

Cerebral amyloid angiopathy (CAA) is recognized as an important cause of lobar intracerebral hemorrhage (ICH) and microbleeds (MBs) in older people ⁽¹⁻⁴⁾. It is a disease in which A β plaques deposited on the blood vessel walls in the brain may lead to stroke ⁽⁵⁾. Amyloid-staining deposits in blood vessels are commonly composed of 39-43 amino acid peptides similar to that of Alzheimer-related senile plaques ⁽⁶⁾. There is a close relationship between CAA and Alzheimer's disease (AD) and they share the same genetic risk factors ^(7, 8). CAA has a prevalence of 78-98% in individuals with AD, but only 25% of patients with AD showed moderate to severe CAA ^(9, 10). CAA may occur in the absence of AD. A recent report on the autopsy of brains of individuals with AD or AD-related pathology (ADRP) showed that the presence of CAA might contribute to neurodegeneration in AD ⁽¹¹⁾. Additionally, it is likely that A β plaques may accumulate earlier in blood vessel walls as well as within the parenchyma. The A β plaques may exist inside and outside the endothelial. Therefore, it is important to develop a non-invasive method for mapping A β plaques accumulating outside the endothelial of cerebral blood vessels. Imaging A β plaques in CAA will allow an improved understanding of A β aggregation and deposition in the cerebral blood vessels, supporting development of both diagnostic and therapeutic agents.

In the past decades, several Positron Emission Tomography (PET) radiopharmaceuticals targeting amyloid plaques in patients have been reported, including florbetapir (Amyvid; [¹⁸F]AV-45, K_i = 2.87 nM) ⁽¹²⁻¹⁶⁾, florbetaben (Neuraceq; [¹⁸F]BAY94-9172, K_i = 2.22 nM) ⁽¹⁷⁻²⁰⁾, and flutemetamol (Vizamyl; [¹⁸F]GE-067, K_i =

Imaging A β Plaques in Cerebral Amyloid Angiopathy

0.74 nM)⁽²¹⁻²⁴⁾ (Figure 1). Recent reports showed that amyloid imaging agents, such as ¹¹C labeled Pittsburgh Compound B (PiB), could image A β plaques in the blood vessels of CAA patients⁽²⁵⁻³¹⁾ (Figure 1). However, ¹¹C-PIB binds to the A β aggregates located in both blood vessels and parenchymal brain tissues, therefore further improvements for selective β -amyloid imaging tracers associated with CAA are necessary for accurately mapping A β aggregates in blood vessels. New ^{99m}Tc(CO)₃ labeled benzothiazole derivatives were reported to show selective binding to A β deposits located in cerebral arterioles⁽³²⁾.

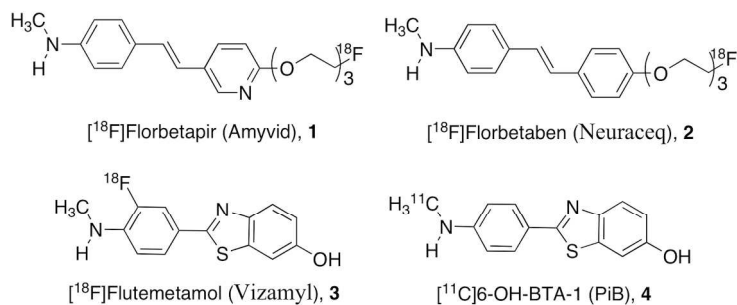


Figure 1. Chemical structures of various PET ligands targeting A β plaques in the brain.

Recently, many advances have been reported with respect to the binding affinity enhancements that were achieved through multivalent binding⁽³³⁻³⁵⁾. Multivalent binding relies on multivalent ligand receptor interactions, which allow multiple and simultaneous binding to several receptors^(36, 37). The self-assembled β -sheet strain of peptides displays multiple and identically spaced binding sites toward the surface of the amyloid fibrils. Thus, multivalency may be useful for enhancing the binding affinity of the molecular imaging ligand for A β aggregates. Iikuni et al. recently reported ^{99m}Tc-hydroxamamide

Imaging A β Plaques in Cerebral Amyloid Angiopathy

(^{99m}Tc -Ham) complexes with a bivalent ligand, such as [^{99m}Tc]**5**. Data suggests the enhancement of the binding affinity occurs by application of bivalency⁽³⁸⁾ (Figure 2).

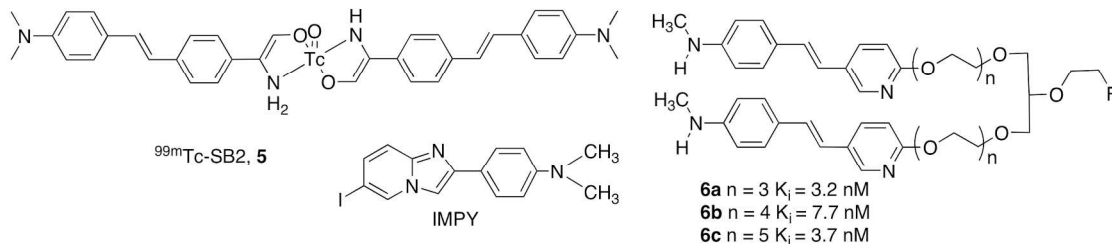


Figure 2. Chemical structures of bivalent ligands and IMPY-targeting A β plaques in the brain. All of the compounds have been previously reported.⁽³⁸⁻⁴⁰⁾

Our group has previously reported ^{18}F -labeled bivalent ligands (**6a-c**) containing multiple AV-45 (styrylpyridine) binding cores, which provided selective detection of A β aggregates in blood vessel walls⁽³⁹⁾ (Figure 2). The binding affinity was measured using postmortem AD brain homogenates against [^{125}I]6-iodo-2-(4'-dimethylamino-)phenyl-imidazo[1,2-a]pyridine ([^{125}I]IMPY)⁽⁴⁰⁾. It is assumed that the styrylpyridine moieties are responsible for inserting into the binding sites within the A β plaques. This bivalency, using two styrylpyridines, will likely improve binding, increase the molecular weight, and reduce the ability to penetrate intact blood-brain barrier (BBB) while targeting the binding to A β plaques only on the blood vessel walls.

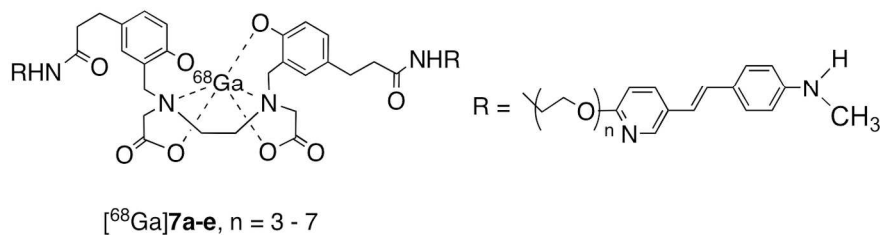
^{68}Ga ($t_{1/2} = 68$ min, $\beta^+ = 89\%$) is an attractive isotope for PET imaging due to its promising physical characteristics and distinctive advantage over ^{18}F , the most commonly used radionuclide for PET imaging. The availability and commercialization of ^{68}Ga from a $^{68}\text{Ge}/^{68}\text{Ga}$ generator allows the simple and routine preparation of ^{68}Ga imaging agents

Imaging A β Plaques in Cerebral Amyloid Angiopathy

without the need of a nearby cyclotron for production. *N,N'*-bis[2-hydroxy-5-(carboxyethyl)benzyl]ethylenediamine-*N,N'*-diacetic acid (HBED-CC) is a highly effective complexing agent for Fe(III) and Ga(III), which forms complexes with $\log K_d = 39.7$ and 39.6 , respectively⁽⁴¹⁾. ^{68}Ga HBED-CC-Ahx-Lys-urea-Glu complexes have been widely used in humans for imaging prostate-specific membrane antigen^(42, 43). The resulting ^{68}Ga HBED-CC derivatives are sufficiently bulky, therefore they can not cross the BBB.

We envision that ^{68}Ga labeled agents targeting A β plaques may provide several advantages: a) the selected HBED-CC core derivatized with styrylpyridinyl groups, allows bivalent binding of A β plaques; b) the ^{68}Ga complex will not penetrate BBB and stay outside the brain parenchymal for binding of A β aggregates on the blood vessel walls; c) ^{68}Ga complex can be readily prepared in minutes using simplified kit formulation; d) ^{68}Ga is a generator-based isotope: it can be made widely available without the need of a nearby cyclotron. Therefore, successful ^{68}Ga CAA imaging agents may lead a widespread clinical application.

On the basis of using bivalent styrylpyridines and ^{68}Ga HBED-CC complexes, we herein report the development and evaluation of several ^{68}Ga -labeled β -amyloid-targeted PET imaging agents, [^{68}Ga]7a-e, for CAA (Figure 3).



Imaging A β Plaques in Cerebral Amyloid Angiopathy

1
2
3
4
5
6
7 Figure 3. Structure of bivalent ligands [^{68}Ga]7a-e, based on styrylpyridine cores. The
8
9 novel compounds are designed to bind to A β aggregates via multiple binding sites.
10
11
12
13
14
15
16
17
18
19
20
21
22
23
24
25
26
27
28
29
30
31
32
33
34
35
36
37
38
39
40
41
42
43
44
45
46
47
48
49
50
51
52
53
54
55
56
57
58
59
60

Imaging A β Plaques in Cerebral Amyloid Angiopathy

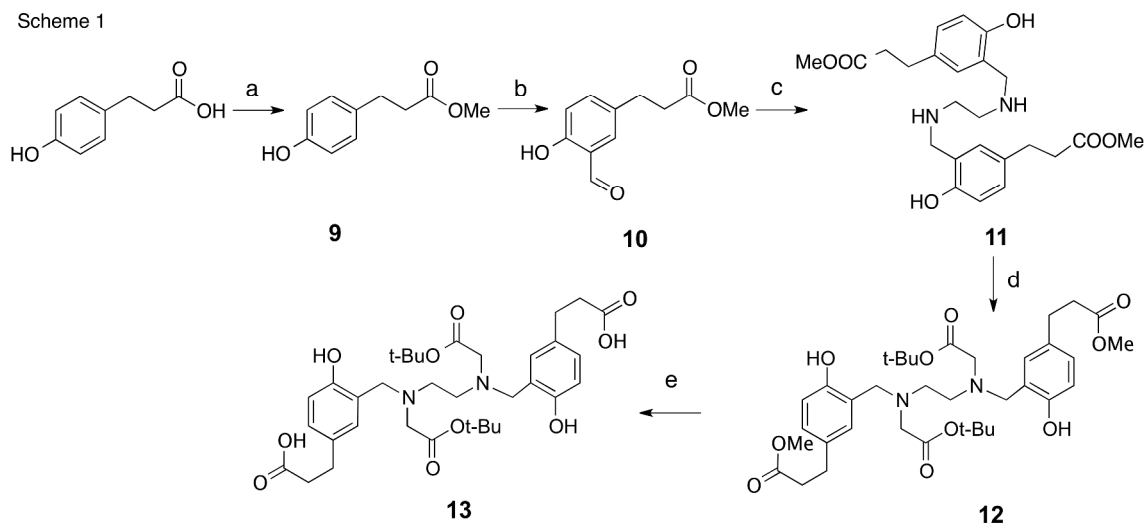
Results

Chemistry. The synthesis of ^{nat}Ga styrylpyridine complexes is summarized in Schemes 1-3. Compound **9** was prepared by O-methylation (esterification) of carboxylic acids in good yield (84%). The methyl ester was treated with MgCl_2 and paraformaldehyde to give salicylaldehyde, **10**, in excellent yield (90%). Condensation of salicylaldehyde with ethylenediamine produced Schiff base without need for further purification. The corresponding secondary amine, **11**, was obtained from the Schiff base after a reduction reaction with sodium borohydride in 69% yield. The secondary amines were condensed with an excess amount of *tert*-butyl bromoacetate to afford **12** in 87% yield. The methyl ester group of compound **12** was selectively removed by NaOH hydrolysis to give acid, **13**, in 96% yield.

The intermediates **21a-e** and **22** were synthesized by a coupling reaction of **13** with the corresponding styrylpyridine, **20a-e**, in 29-59% yield. The *tert*-butyl and Boc protection groups were then removed by trifluoroacetic acid (TFA) to give **7a-e** and **8** in 28-44% yield. The precursors, **7a-e** and **8**, were used for radiolabeling and for the synthesis of “cold compounds” ^{nat}Ga **7a-e** and ^{nat}Ga **8**.

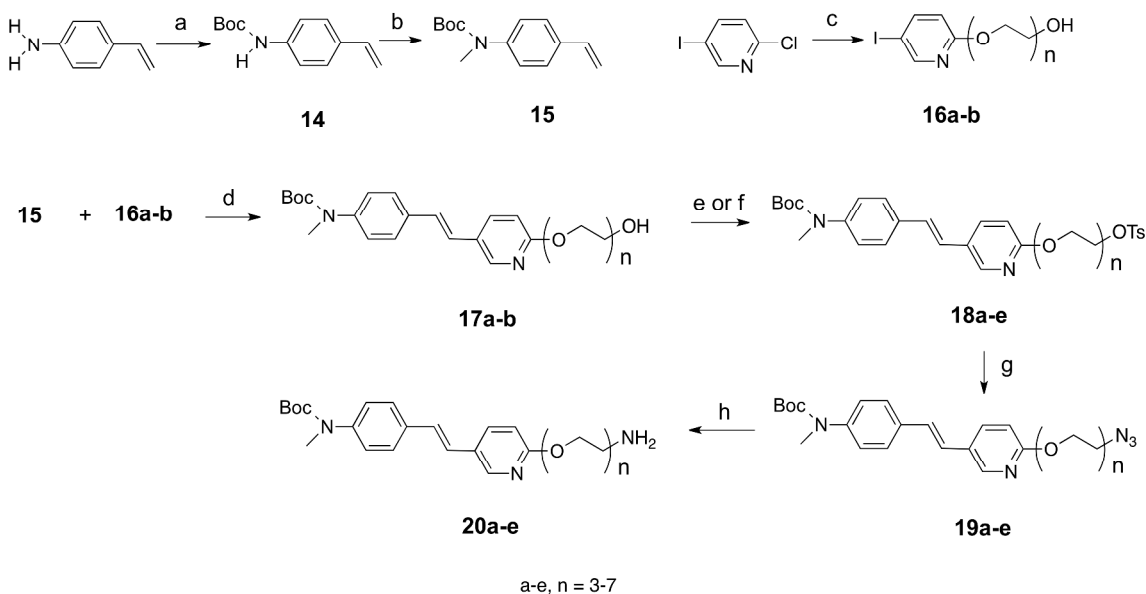
Imaging A β Plaques in Cerebral Amyloid Angiopathy

Scheme 1



Reagent and conditions: (a) MeOH, $\text{BF}_3 \cdot \text{Et}_2\text{O}$, rt; (b) $(\text{CHO})_n$, MgCl_2 , Et_3N , ACN, reflux; (c) ethylenediamine, NaBH_4 , MeOH, 50 °C, rt; (d) tert-Butyl bromoacetate, Na_2CO_3 , ACN, 60 °C; (e) NaOH, MeOH, H_2O , rt.

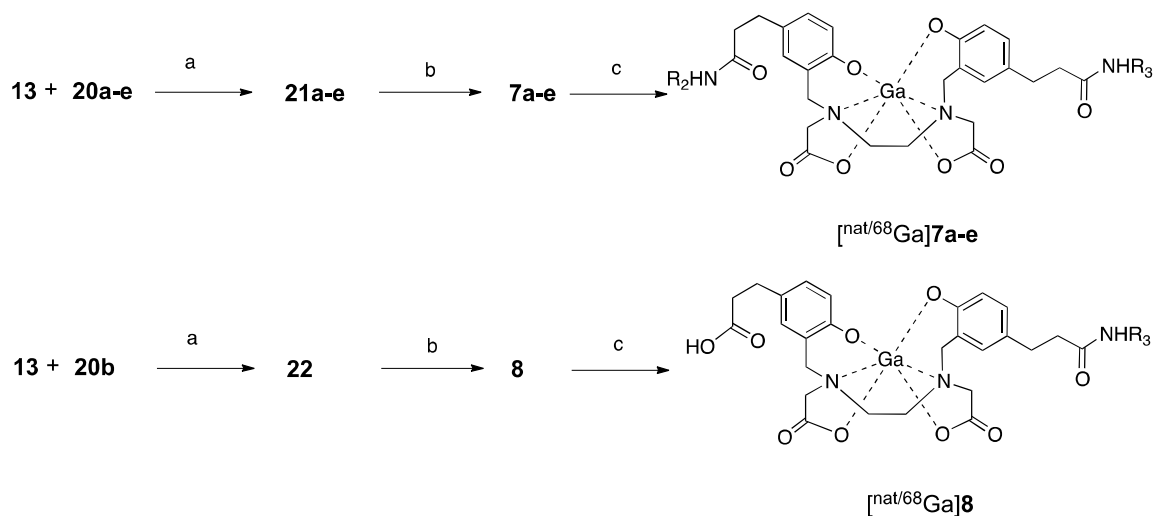
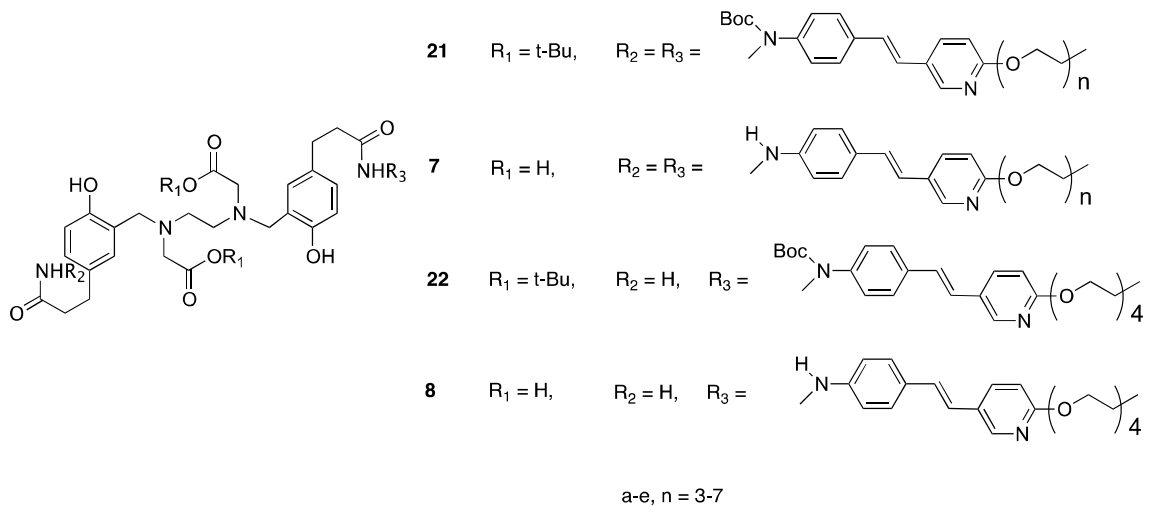
Scheme 2



Reagent and conditions: (a) $(\text{Boc})_2\text{O}$, H_2O , 35 °C; (b) NaH, CH_3I , DMF, rt; (c) triethylene glycol or tetraethylene glycol, Cs_2CO_3 , DMF, 150 °C; (d) K_2CO_3 , Bu_4NBr , $\text{Pd}(\text{OAc})_2$, DMF, 60 °C; (e) TsCl, Et_3N , DMAP, DCM, rt; (f) diethylene glycol ditosylate or triethylene glycol ditosylate, NaH, DMF, rt; (g) NaN_3 , DMF, 60 °C; (h) PPh_3 , H_2O , THF, 68 °C.

Imaging A β Plaques in Cerebral Amyloid Angiopathy

Scheme 3



Reagent and conditions: (a) EDCI, HOBT, DIPEA, DMF, rt; (b) TFA, rt; (c) [^{68}Ga]GaCl $_3$, H $_2$ O, rt.

Radiosynthesis of [^{68}Ga]7a-e and [^{68}Ga]8. ^{68}Ga conjugates were readily prepared by incubating an excess of corresponding starting materials, **7a-e** or **8** ($\sim 20 \mu\text{M}$), with [^{68}Ga]GaCl $_4^-$ (2.5-3.0 mCi in 0.05 N HCl, obtained from a $^{68}\text{Ge}/^{68}\text{Ga}$ generator) and NaOAc buffer, resulting in specific activities ranging from 236 to 283 Ci/mmol. The labeling efficiency of ^{68}Ga conjugates was greater than 93%, as confirmed by TLC and HPLC analysis. TLC with citric acid showed $R_f = 0$ for ^{68}Ga conjugates and ^{68}Ga colloid

Imaging A β Plaques in Cerebral Amyloid Angiopathy

and $R_f = 0.9-1.0$ for free of $[^{68}\text{Ga}]\text{GaCl}_4^-$. In the second solvent system, ^{68}Ga conjugates migrated to the solvent front, whereas the expected $[^{68}\text{Ga}]\text{GaCl}_4^-$ and ^{68}Ga colloid stayed at the origin. The retention times obtained for each compound from HPLC were identical to authentic “cold” standards. The $[^{68}\text{Ga}]\mathbf{7a-e}$ and $[^{68}\text{Ga}]\mathbf{8}$ preparations were found to be stable for more than 3 h at room temperature (rt) in phosphate-buffered saline (PBS). Furthermore, no significant degradation of any ^{68}Ga conjugates was observed up to 3 h post-preparation, when incubated with human plasma at 37 °C, thus suggesting high *in vitro* stability.

In vitro binding studies using A β -aggregates in the AD brain tissue homogenates. An *in vitro* competitive binding assay was conducted to measure the inhibition of $[^{125}\text{I}]\text{IMPY}$, a known A β -aggregates ligand⁽⁴⁴⁾, binding to A β -aggregates in the AD brain tissue homogenates. Inhibition constants (K_i , nM) of various ligands (free ligands and $^{\text{nat}}\text{Ga}$ conjugates) against the binding of $[^{125}\text{I}]\text{IMPY}$ to A β -aggregates are shown in Table 1. The HBED-based bivalent ligands (**7a-e**) displayed high binding affinities ($K_i = 1.80, 3.53, 4.52, 1.52$ and 1.71 nM, respectively), whereas the associated $^{\text{nat}}\text{Ga}$ conjugates showed lower binding affinities ($K_i = 30.6, 13.4, 18.1, 6.70$ and 10.7 nM, respectively) (Table 1). The length of the pegylation chain showed no remarkable effect on the binding affinities. However, the monovalent ligands showed dramatically lower binding affinities (**8** and $[^{\text{nat}}\text{Ga}]\mathbf{8}$, $K_i = 239$ and 185 nM, respectively). These monovalent Ga conjugates were not studied any further.

Table 1. Inhibition constant (K_i , nM) of A β plaques targeting styrylpyridine derivatives against binding of $[^{125}\text{I}]\text{IMPY}$, a known A β -aggregates ligand⁽⁴⁴⁾

Compound Name	K_i (nM)*	Compound Name	K_i (nM)*
---------------	-------------	---------------	-------------

Imaging A β Plaques in Cerebral Amyloid Angiopathy

7a (n = 3)	1.80 \pm 0.24	[^{nat} Ga]7a (n = 3)	30.6 \pm 6.97
7b (n = 4)	3.53 \pm 1.21	[^{nat} Ga]7b (n = 4)	13.4 \pm 3.71
7c (n = 5)	4.52 \pm 2.42	[^{nat} Ga]7c (n = 5)	18.1 \pm 4.32
7d (n = 6)	1.52 \pm 0.20	[^{nat} Ga]7d (n = 6)	6.70 \pm 1.70
7e (n = 7)	1.71 \pm 0.25	[^{nat} Ga]7e (n = 7)	10.7 \pm 4.45
8	239 \pm 38	[^{nat} Ga]8a	185 \pm 80
florbetapir (AV-45), 1	2.87 \pm 0.17		
*Measured against [¹²⁵ I]IMPY binding to A β plaques in postmortem AD brain homogenates, n= 3.			

In vitro autoradiography of AD brain sections. The postmortem AD brain sections containing A β plaques were labeled intensely by all of the bivalent ligands, [⁶⁸Ga]7a-e. The adjacent sections were labeled by [¹²⁵I]IMPY and showed different images to those of [⁶⁸Ga]7a-e (Figure 4). Furthermore, the autoradiographic signals were almost completely blocked after incubating the sections in the presence of excess of IMPY (28 μ M), demonstrating [⁶⁸Ga]7a-e were competing for the same A β plaque binding sites. As expected, the monovalent ligand, [⁶⁸Ga]8, did not show any A β plaques labeling, which was consistent with the low binding affinity measured by an *in vitro* binding assay using AD brain homogenates.

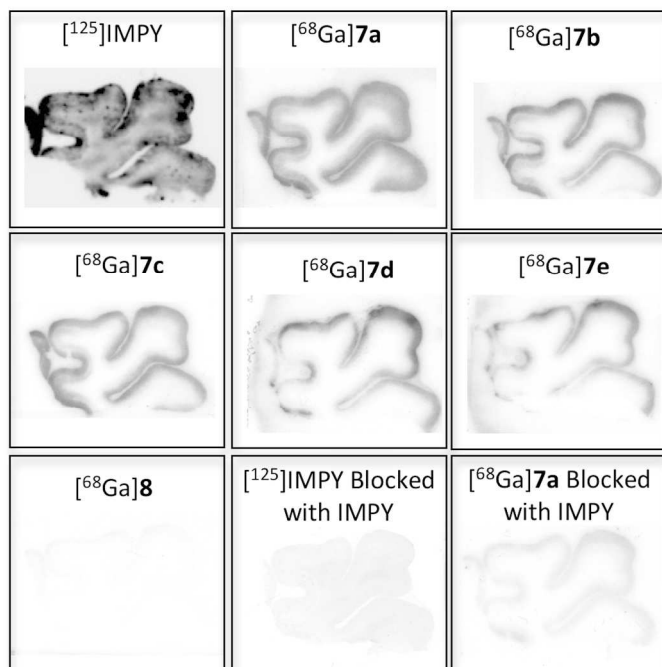
Imaging A β Plaques in Cerebral Amyloid Angiopathy

Figure 4. *In vitro* autoradiography of brain sections from AD patients labeled with [^{125}I]IMPY, [^{68}Ga]7a-e, and [^{68}Ga]8. [^{125}I]IMPY and [^{68}Ga]7a binding in AD brain sections blocked in the presence of 28 μM IMPY.

In vivo biodistribution study in CD-1 mice. After an iv injection in normal mice, [^{68}Ga]7a-e showed low brain uptake (0.1–0.3% ID/g at 2 min post injection) (table 2). Compared to the brain uptake of [^{18}F]1, the bivalent ligands, [^{68}Ga]7a-e, clearly displayed a very low brain penetration. This may allow a selective labeling of A β plaques deposited on the walls of cerebral blood vessels, not in the A β plaques in the parenchymal brain tissues.

Table 2. Biodistribution in normal CD-1 mice after an iv injection of [^{68}Ga]7a-e and [^{68}Ga]8 in saline (% dose/g, n = 3)

Imaging A β Plaques in Cerebral Amyloid Angiopathy

	[⁶⁸ Ga]7a		[⁶⁸ Ga]7b	
organ	2 min	60 min	2 min	60 min
blood	3.10 ± 0.27	0.88 ± 0.15	4.57 ± 0.07	0.59 ± 0.82
muscle	0.26 ± 0.02	0.15 ± 0.11	0.47 ± 0.10	0.15 ± 0.04
kidney	3.71 ± 0.33	1.87 ± 0.52	4.94 ± 0.44	1.97 ± 0.13
liver	25.7 ± 3.25	22.5 ± 2.63	28.5 ± 3.24	15.4 ± 1.07
brain	0.12 ± 0.05	0.08 ± 0.09	0.17 ± 0.05	0.04 ± 0.00
bone	0.48 ± 0.04	0.40 ± 0.08	0.74 ± 0.12	0.44 ± 0.11
	[⁶⁸ Ga]7c		[⁶⁸ Ga]7d	
organ	2 min	60 min	2 min	60 min
blood	9.48 ± 3.63	7.24 ± 4.21	7.85 ± 1.95	2.35 ± 0.54
muscle	0.68 ± 0.18	0.35 ± 0.03	0.42 ± 0.07	0.34 ± 0.05
kidney	10.7 ± 2.09	3.32 ± 0.23	4.01 ± 0.11	2.03 ± 0.10
liver	43.3 ± 17.8	26.7 ± 2.43	15.9 ± 0.61	12.8 ± 1.80
brain	0.31 ± 0.09	0.11 ± 0.03	0.21 ± 0.05	0.11 ± 0.01
bone	1.02 ± 0.34	0.82 ± 0.13	0.98 ± 0.03	0.74 ± 0.08
	[⁶⁸ Ga]7e		[⁶⁸ Ga]8	
organ	2 min	60 min	2 min	60 min
blood	6.87 ± 0.86	2.88 ± 0.64	3.22 ± 0.44	1.01 ± 0.10
muscle	0.41 ± 0.05	0.35 ± 0.05	0.40 ± 0.03	0.14 ± 0.01
kidney	4.75 ± 0.24	2.40 ± 0.41	6.33 ± 0.65	1.63 ± 0.12
liver	12.6 ± 0.86	8.12 ± 0.31	23.3 ± 2.06	2.17 ± 0.24
brain	0.22 ± 0.03	0.07 ± 0.01	0.11 ± 0.01	0.03 ± 0.00
bone	0.75 ± 0.08	0.46 ± 0.02	0.57 ± 0.11	0.26 ± 0.03

Imaging A β Plaques in Cerebral Amyloid Angiopathy

Discussion

In the present study, we reported a series of novel ^{68}Ga -HBED complexes containing bivalent polypegylated styrylpyridine as PET imaging agents for mapping A β plaques in the blood vessels of CAA patients. They are useful as alternatives to ^{18}F labeled imaging agents. Compared to ^{18}F , ^{68}Ga is more conveniently produced by $^{68}\text{Ge}/^{68}\text{Ga}$ generators without an on-site cyclotron. In addition, ^{68}Ga provides a simple, rapid radiolabeling method, which is suitable for using a convenient lyophilized kit formulation⁽⁴⁵⁾. Many potential chelating agents have been reported for complexation of ^{68}Ga to targeted carrier molecules⁽⁴⁶⁾. The predominantly used bifunctional ^{68}Ga chelator is 1,4,7,10-tetraazacyclododecane-1,4,7,10-tetraacetic acid (DOTA), and it is considered the “gold standard” for chelating radioactive metals^(47, 48). However, ^{68}Ga complexation with DOTA requires heating at elevated temperatures or longer reaction times, which might have detrimental effects on heat-labile ligands such as proteins or other biomolecules. Therefore other chelators such as 1,4,7-triazacyclononane-triacetic acid (NOTA) and (2,2-(7-(1-carboxy-4-(2-mercaptoethylamino)-4-oxobutyl)-1,4,7-triazonane-1,4-diyl)diacetic acid) (NODAGA) have been evaluated to circumvent these problems⁽⁴⁹⁾^(50, 51). Among them, HBED was described recently as a highly efficient chelator allowing fast and easy-to-perform labeling at room temperature⁽⁵²⁾. Previously reported synthesis of HBED complexes employed a Fe complex of HBED-CC as the intermediate⁽⁵³⁾. The reaction scheme was relatively inefficient, and a new scheme involving a more efficient, simpler means to carry out, without the use of Fe(III) HBED-CC complex was described in Scheme 1. As described here, the ^{68}Ga complexation of all ligands, [^{68}Ga]7a-e and [^{68}Ga]8, resulted in high radiochemical yields of 93-98% after 5 min reaction time at

Imaging A β Plaques in Cerebral Amyloid Angiopathy

room temperate, which led to less than 20 min of preparation time for radiolabeling and quality control. As a consequence, radiotracers were subsequently used for *in vitro* and *in vivo* experiments without further purification. All ^{68}Ga conjugates used in this study proved to be stable in PBS and human plasma for the study-relevant time period of 3 h.

One of the major pre-requisites for the function of the chelator in radiopharmaceuticals is that the structure and physical properties of the metal complex do not have a large impact on receptor binding⁽⁴⁶⁾. The change of overall charge and lipophilicity of the radiometal complexes often influence pharmacokinetics of targeting moiety, especially for small vectors. The HBED-CC styrylpyridines showed the desired high binding affinity comparable to that of [^{18}F]AV-45 ([^{18}F]1)^(13, 14) and previously reported ^{18}F -labeled CAA imaging agents ([^{18}F]6a-c). We also developed other ^{68}Ga complexes with different chelating groups, such as DOTA and 6-amino-6-methylperhydro-1,4-diazepinetetraacetic acid (AAZTA)^(54, 55), to compare with [^{68}Ga]7a-c in terms of β -amyloid binding characteristics. Surprisingly, compared to the HBED complexes [^{68}Ga]7a-c, the DOTA and AAZTA complexes showed significantly lower binding affinities (data not shown). This decrease may have been caused by the change of hydroxybenzyl groups of the ligands. Further investigations with other chelating groups such as NOTA, NODAGA, and 2-[[6-(carboxy)-pyridin-2-yl]-methylamino]ethane (H₂dedpa) will be required to confirm the validity of this assumption.

Various multivalent ligands have been reported for enhancing peptide affinity⁽³³⁾. An interesting study comparing binding affinity with amyloid aggregates between bivalent and monovalent ligands showed that the bivalent scaffold correlates with

Imaging A β Plaques in Cerebral Amyloid Angiopathy

1
2
3 improved binding ⁽³⁸⁾. For this report, we have prepared and examined the A β aggregate
4 binding affinity of HBED-CC styrylpyridines, **7a-e**, **8**, and corresponding ^{nat}Ga
5 conjugates. Similarly, the high binding affinities observed for bivalent ligands (**7a-e**
6 (dimer), $K_i = 1.7-4.5$ nM vs. **8** (monovalent), $K_i = 239$ nM), suggest that there are
7 bivalent interactions in binding to neighboring binding sites, and a bivalent ligand shows
8 better binding affinity than the comparable monomer. The comparison of the inhibition
9 constants of **7a-e** suggested the length of the PEG scaffold did not interfere with the
10 binding. However, the binding affinity of Ga conjugates, [^{nat}Ga]**7a-e**, showed a slight
11 reduction ($K_i = 6-30$ nM), compared to the precursors. This indicates that the change of
12 geometry after ^{nat}Ga complex formation might change the interaction with aggregated
13 amyloid peptides and reduce the binding affinity.
14
15
16
17
18
19
20
21
22
23
24
25
26
27
28
29

30
31 *In vitro* labeling of A β plaques in AD brain sections showed that [⁶⁸Ga]**7a-e** were
32 capable of labeling A β aggregates in brain sections, indicating the feasibility of using
33 them as PET imaging agents for detecting A β plaques in CAA patients. Of note, whereas
34 [¹²⁵I]IMPY exhibited a discrete binding pattern, [⁶⁸Ga]**7a-e** displayed a more blurry
35 image. Presumably, this discrepancy is due to lower auger electrons from ¹²⁵I and the
36 relatively longer traveling distance of positrons emitted by ⁶⁸Ga. As expected, [⁶⁸Ga]**8**
37 showed no marked labeling to A β plaques. The data of *in vitro* autoradiography of AD
38 brain sections are consistent with those of *in vitro* binding studies.
39
40
41
42
43
44
45
46
47
48
49

Conclusion

50
51
52
53
54 A new series of ⁶⁸Ga-HBED-CC conjugates with bivalent styrylpyridine targeting
55 A β aggregates on the walls of blood vessels was successfully prepared and tested. The
56
57
58
59
60

Imaging A β Plaques in Cerebral Amyloid Angiopathy

1
2
3 bivalent ligands, [⁶⁸Ga]**7a-e**, showed highly promising A β aggregate-binding affinity.
4
5 The enhancement of binding affinity was confirmed by *in vitro* autoradiography of
6
7 postmortem AD brain sections. Furthermore, [⁶⁸Ga]**7a-e** displayed low BBB penetration,
8
9 showing low uptake in the brains of normal mice. These results support that similar to
10
11 [¹⁸F]**6a-c** ⁽³⁹⁾, [⁶⁸Ga]**7a-e** are equally effective and are considered as promising candidates
12
13 for PET imaging agents for A β plaques on the walls of blood vessels in CAA.
14
15
16
17
18
19
20
21
22
23
24
25
26
27
28
29
30
31
32
33
34
35
36
37
38
39
40
41
42
43
44
45
46
47
48
49
50
51
52
53
54
55
56
57
58
59
60

Imaging A β Plaques in Cerebral Amyloid Angiopathy

Experimental sections

General. All chemicals were purchased from Aldrich Chemical Co. and used without further purification unless otherwise indicated. Solvents were dried through a molecular sieve system (Pure Solve Solvent Purification System; Innovative Technology, Inc.). Normal CD-1 mice (20-26 g) were used for the biodistribution studies. The protocol requiring the use of mice was reviewed and approved by the Institutional Animal Care and Use Committee (University of Pennsylvania). Postmortem human samples were obtained from the National Disease Research Interchange (NDRI, Philadelphia, PA).

The synthesis of bivalent and monovalent styrylpyridine derivatives, **7a-e** and **8**, was outlined in Schemes 1-3. The details of the procedure for synthesis of **14-20** are included in the supplemental information.

Chemistry. Methyl 3-(4-hydroxyphenyl)propanoate (9). To a solution of 3-(4-hydroxyphenyl)propanoic acid (3.0 g, 18.1 mmol) in 50 mL MeOH was added BF₃•Et₂O (0.3 mL). After stirring at rt for 6 h, the solvent was removed, and the residue was purified by flash chromatography (FC) (ethyl acetate (EtOAc)/hexane = 2/8) to give **9** as a white solid (yield: 2.72 g, 83.5%). ¹HNMR (400 MHz, CDCl₃) δ : 7.07(d, 2H, J = 8.4 Hz), 6.76 (d, 2H, J = 8.4 Hz), 4.72 (s, 1H), 3.68 (s, 3H), 2.89 (t, 2H, J = 7.6 Hz), 2.60 (t, 2H, J = 7.6 Hz); HRMS calcd. for C₁₀H₁₃O₃ (M + H)⁺: 181.0865, found 181.0815.

Methyl 3-(3-formyl-4-hydroxyphenyl)propanoate (10). To a solution of **9** (2.72 g, 15.1 mmol) in 70 mL acetonitrile (ACN), MgCl₂ (2.87 g, 30.2 mmol),

Imaging A β Plaques in Cerebral Amyloid Angiopathy

1
2
3 paraformaldehyde (3.66 g, 120.8 mmol), and triethylamine (Et₃N, 6.1 g, 60.4 mmol) were
4
5 added at rt. The mixture was heated under reflux for 8 h, diluted with water (25 mL),
6
7 followed by acidification using HCl (5%, 100 mL), and extraction with ether (50 mL \times
8
9 3). The organic layer was then dried over MgSO₄ and filtered. The filtrate was
10
11 concentrated, and the residue was purified by FC (EtOAc/hexane = 2/8) to give **10** as a
12
13 white solid (yield: 2.85 g, 90.4%). ¹HNMR (400 MHz, CDCl₃) δ : 10.89 (s, 1H), 9.88 (s,
14
15 1H), 7.37-7.40 (m, 2H), 6.94 (d, 1H, J = 9.6 Hz), 3.68 (s, 3H), 2.95 (t, 2H, J = 7.4 Hz),
16
17 2.64 (t, 2H, J = 7.4 Hz); HRMS calcd. for C₁₁H₁₃O₄ (M + H)⁺: 209.0814, found
18
19 209.0825.
20
21
22
23
24
25

26 **Dimethyl 3,3'-(((ethane-1,2-diylbis(azanediyl))bis(methylene))bis(4-hydroxy-**
27
28 **3,1-phenylene))dipropanoate (11).** Ethylenediamine (0.371 g, 6.18 mmol) was added to
29
30 a solution of **10** (2.84 g, 13.6 mmol) in 60 mL MeOH at rt. After stirring at 50 °C
31
32 overnight, the mixture was cooled in an ice-bath. NaBH₄ (1.05 g, 27.81 mmol) was added
33
34 in portions to the reaction mixture, and the resulting solution was allowed to warm to rt.
35
36 After being stirred at rt for 24 h, the reaction was quenched with 100 mL H₂O and
37
38 extracted with ethyl acetate (150 \times 3 mL). The organic layer was dried over MgSO₄ and
39
40 filtered. The filtrate was then concentrated, and the residue was purified by FC
41
42 (dichloromethane (DCM)/MeOH/NH₄OH = 90/9/1) to give **11** as a colorless oil (yield:
43
44 2.08 g, 68.8%). ¹HNMR (400 MHz, CDCl₃) δ : 7.00 (dd, 2H, J = 2.0 Hz, J = 8.4 Hz), 6.82
45
46 (d, 2H, J = 2.0 Hz), 6.76 (d, 2H, J = 8.4 Hz), 3.97 (s, 4H), 2.67 (s, 6H), 2.83-2.87 (m,
47
48 8H), 2.58 (t, 4H, J = 7.8 Hz); HRMS calcd. for C₂₄H₃₃N₂O₆ (M + H)⁺: 445.2339, found
49
50 445.2139.
51
52
53
54
55
56
57
58
59
60

Imaging A β Plaques in Cerebral Amyloid Angiopathy

1
2
3 **Dimethyl** **3,3'-(((2,2,13,13-tetramethyl-4,11-dioxo-3,12-dioxa-6,9-**
4
5
6 **diazatetradecane-6,9-diyl)bis(methylene))bis(4-hydroxy-3,1-**
7
8 **phenylene))dipropanoate (12).** To a solution of **11** (1.8 g, 4.05 mmol) in 50 mL ACN,
9
10 *tert*-Butyl bromoacetate (1.66 g, 8.51 mmol) and Na₂CO₃ (1.71 g, 16.2 mmol) were
11
12 added. The mixture was then heated at 60 °C overnight before being cooled to rt and
13
14 filtered. The filtrate was concentrated, and the residue was purified by FC (EtOAc/hexane
15
16 = 1/1) to give **12** as a colorless oil (yield: 2.36 g, 86.6%). ¹HNMR (400 MHz, CDCl₃) δ :
17
18 9.55 (s, 2H), 7.00 (dd, 2H, *J* = 2.0 Hz, *J* = 8.4 Hz), 6.77 (d, 2H, *J* = 8.4 Hz), 6.74 (d, 2H,
19
20 *J* = 2.0 Hz), 3.70 (s, 4H), 3.67 (s, 6H), 3.17 (s, 4H), 2.83 (t, 4H, *J* = 7.8 Hz), 2.69 (s, 4H),
21
22 2.57 (t, 4H, *J* = 7.8 Hz), 1.46 (s, 18H); HRMS calcd. for C₃₆H₅₃N₂O₁₀ (M + H)⁺:
23
24 673.3700, found 673.3662.
25
26
27
28
29

30 **3,3'-(((2,2,13,13-Tetramethyl-4,11-dioxo-3,12-dioxa-6,9-diazatetradecane-6,9-**
31
32 **diyl)bis(methylene))bis(4-hydroxy-3,1-phenylene))dipropanoic acid (13).** A solution
33
34 of **12** (1.6 g, 2.38 mmol) in 10 mL MeOH/NaOH (1 N) (1/1) was stirred at rt for 2 h. HCl
35
36 (1 N) was then added to the reaction mixture to pH = 4-5. The resulting mixture was
37
38 extracted with EtOAc (50 mL \times 3). The organic layer was then dried over MgSO₄ and
39
40 filtered. The filtrate was concentrated, and the residue was purified by FC
41
42 (DCM/MeOH/NH₄OH = 90/9/1) to give **13** as a white solid (yield: 1.2 g, 78.2%).
43
44 ¹HNMR (400 MHz, CDCl₃) δ : 7.03 (dd, 2H, *J* = 2.0 Hz, *J* = 8.4 Hz), 6.80 (d, 2H, *J* = 8.4
45
46 Hz), 6.71 (d, 2H, *J* = 2.0 Hz), 3.56 (s, 4H), 3.26 (s, 4H), 2.84 (t, 4H, *J* = 7.0 Hz), 2.62 (t,
47
48 4H, *J* = 7.0 Hz), 2.56 (s, 4H), 1.48(s, 18H); HRMS calcd. for C₃₄H₄₉N₂O₁₀ (M + H)⁺:
49
50 645.3387, found 645.3417.
51
52
53
54
55
56
57
58
59
60

Imaging A β Plaques in Cerebral Amyloid Angiopathy

Di-tert-butyl 2,2'-((E)-ethane-1,2-diylbis((5-(3-((2-(2-((5-((E)-4-((tert-butoxycarbonyl)(methyl)amino)styryl)pyridin-2-yl)oxy)ethoxy)ethoxy)ethyl)amino)-3-oxopropyl)-2-hydroxybenzyl)azanediyl))diacetate (21a). To a solution of **13** (118.3 mg, 0.183 mmol) in 5 mL DMF, *N,N*-diisopropylethylamine (DIPEA, 189.6 mg, 1.47 mmol), 1-hydroxybenzotriazole hydrate (HOBt, 0.55 mmol, 92.8 mg), *N*-(3-dimethylaminopropyl)-*N*-ethylcarbodiimide hydrochloride (EDC, 105 mg, 0.55 mmol) and **20a** (168 mg, 0.367 mmol) were added at 0 °C. The mixture was stirred at rt for overnight before 30 mL EtOAc was added to the reaction mixture. It was then washed with H₂O (10 mL \times 2) and brine (10 mL), dried over MgSO₄, and filtered. The filtrate was concentrated, and the residue was purified by FC (DCM/MeOH/NH₄OH = 95/5/0.5) to give **21a** as a colorless oil (yield: 140 mg, 50.2%): ¹HNMR (400 MHz, CDCl₃) δ : 9.50 (br s, 2H), 8.17 (d, 2H, *J* = 2.4 Hz), 7.78 (dd, 2H, *J* = 2.4 Hz, *J* = 8.8 Hz), 7.45 (d, 4H, *J* = 8.8 Hz), 7.24 (d, 4H, *J* = 8.4 Hz), 6.97-7.02 (m, 6H), 6.73-6.77 (m, 6H), 6.23 (br s, 2H), 4.50 (t, 4H, *J* = 4.8 Hz), 3.85 (t, 4H, *J* = 4.8 Hz), 3.67-3.73 (m, 12H), 3.53 (t, 4H, *J* = 5.0 Hz), 3.43 (t, 4H, *J* = 5.2 Hz), 3.28 (s, 6H), 3.18 (s, 4H), 2.84 (t, 4H, *J* = 7.8 Hz), 2.67 (s, 4H), 2.42 (t, 4H, *J* = 7.8 Hz), 1.48 (s, 18H), 1.46 (s, 18H); HRMS calcd. for C₈₄H₁₁₅N₈O₁₈ (M + H)⁺: 1523.8329, found 1523.8373.

Di-tert-butyl 2,2'-((E)-ethane-1,2-diylbis((5-(1-((5-((E)-4-((tert-butoxycarbonyl)(methyl)amino)styryl)pyridin-2-yl)oxy)-13-oxo-3,6,9-trioxa-12-azapentadecan-15-yl)-2-hydroxybenzyl)azanediyl))diacetate (21b). Compound **21b** (yield: 43 mg, 49.5%) was prepared from **13** (43 mg, 0.0667 mmol), DIPEA (68.9 mg, 0.534 mmol), HOBt (33.8 mg, 0.2 mmol), EDC (38.2 mg, 0.2 mmol), and **20b** (67 mg, 0.1334 mmol) following the same procedure described for compound **21a**. ¹HNMR (400

Imaging A β Plaques in Cerebral Amyloid Angiopathy

MHz, CDCl₃) δ : 9.50 (br s, 2H), 8.17 (d, 2H, $J = 2.4$ Hz), 7.77 (dd, 2H, $J = 2.4$ Hz, $J = 8.8$ Hz), 7.44 (d, 4H, $J = 8.8$ Hz), 7.23 (d, 4H, $J = 8.4$ Hz), 6.96-7.00 (m, 6H), 6.73-6.77 (m, 6H), 6.30 (br s, 2H), 4.48 (t, 4H, $J = 4.8$ Hz), 3.84 (t, 4H, $J = 4.8$ Hz), 3.56-3.72 (m, 20H), 3.51 (t, 4H, $J = 5.0$ Hz), 3.40 (t, 4H, $J = 5.2$ Hz), 3.27 (s, 6H), 3.17 (s, 4H), 2.82 (t, 4H, $J = 7.8$ Hz), 2.66 (s, 4H), 2.41 (t, 4H, $J = 7.8$ Hz), 1.46 (s, 18H), 1.45 (s, 18H); HRMS calcd. for C₈₈H₁₂₃N₈O₂₀ (M + H)⁺: 1611.8854, found 1611.8998.

Di-*tert*-butyl 2,2'-((*E*)-ethane-1,2-diylbis((5-(1-((5-((*E*)-4-((*tert*-butoxycarbonyl)(methyl)amino)styryl)pyridin-2-yl)oxy)-16-oxo-3,6,9,12-tetraoxa-15-azaoctadecan-18-yl)-2-hydroxybenzyl)azanediyl)diacetate (21c). Compound **21c** (yield: 40 mg, 51.2%) was prepared from **13** (29.7 mg, 0.046 mmol), DIPEA (47.4 mg, 0.368 mmol), HOBt (23.3 mg, 0.138 mmol), EDC (26.3 mg, 0.138 mmol), and **20c** (50 mg, 0.092 mmol) following the same procedure described for compound **21a**. ¹HNMR (400 MHz, CDCl₃) δ : 9.50 (br s, 2H), 8.17 (d, 2H, $J = 2.0$ Hz), 7.77 (dd, 2H, $J = 2.4$ Hz, $J = 8.8$ Hz), 7.44 (d, 4H, $J = 8.8$ Hz), 7.22 (d, 4H, $J = 8.4$ Hz), 6.96-7.01 (m, 6H), 6.73-6.78 (m, 6H), 6.29 (br s, 2H), 4.47 (t, 4H, $J = 4.8$ Hz), 3.83 (t, 4H, $J = 4.8$ Hz), 3.56-3.71 (m, 28H), 3.50 (t, 4H, $J = 5.0$ Hz), 3.42 (t, 4H, $J = 5.2$ Hz), 3.27 (s, 6H), 3.16 (s, 4H), 2.83 (t, 4H, $J = 7.8$ Hz), 2.66 (s, 4H), 2.41 (t, 4H, $J = 7.8$ Hz), 1.46 (s, 18H), 1.45 (s, 18H); HRMS calcd. for C₉₂H₁₃₁N₈O₂₂ (M + H)⁺: 1699.9378, found 1699.9348.

Di-*tert*-butyl 2,2'-((*E*)-ethane-1,2-diylbis((5-(1-((5-((*E*)-4-((*tert*-butoxycarbonyl)(methyl)amino)styryl)pyridin-2-yl)oxy)-19-oxo-3,6,9,12,15-pentaoxa-18-azahenicosan-21-yl)-2-hydroxybenzyl)azanediyl)diacetate (21d). Compound **21d** (yield: 60 mg, 58.9%) was prepared from **13** (36.8 mg, 0.057 mmol),

Imaging A β Plaques in Cerebral Amyloid Angiopathy

DIPEA (58.8 mg, 0.456 mmol), HOBT (31 mg, 0.187 mmol), EDC (36 mg, 0.187 mmol) and **20d** (67 mg, 0.114 mmol), following the same procedure described for compound **21a**. ¹HNMR (400 MHz, CDCl₃) δ : 9.50 (br s, 2H), 8.17 (d, 2H, $J = 2.0$ Hz), 7.78 (dd, 2H, $J = 2.4$ Hz, $J = 8.8$ Hz), 7.44 (d, 4H, $J = 8.4$ Hz), 7.22 (d, 4H, $J = 8.8$ Hz), 6.96-7.01 (m, 6H), 6.73-6.79 (m, 6H), 6.22 (br s, 2H), 4.48 (t, 4H, $J = 4.8$ Hz), 3.85 (t, 4H, $J = 4.8$ Hz), 3.57-3.71 (m, 36H), 3.50 (t, 4H, $J = 5.0$ Hz), 3.42 (t, 4H, $J = 5.2$ Hz), 3.27 (s, 6H), 3.17 (s, 4H), 2.83 (t, 4H, $J = 7.8$ Hz), 2.66 (s, 4H), 2.41 (t, 4H, $J = 7.8$ Hz), 1.46 (s, 18H), 1.45 (s, 18H); HRMS calcd. for C₉₆H₁₃₉N₈O₂₄ (M + H)⁺: 1787.9902, found 1787.9882.

Di-tert-butyl 2,2'-((E)-ethane-1,2-diylbis((5-(1-((5-((E)-4-((tert-butoxycarbonyl)(methyl)amino)styryl)pyridin-2-yl)oxy)-22-oxo-3,6,9,12,15,18-hexaoxa-21-azatetracosan-24-yl)-2-hydroxybenzyl)azanediyl))diacetate (21e).

Compound **21e** (yield: 83 mg, 55.3%) was prepared from **13** (51.6 mg, 0.08 mmol), DIPEA (82.6 mg, 0.64 mmol), HOBT (40.5 mg, 0.24 mmol), EDC (45.8 mg, 0.24 mmol) and **20e** (100 mg, 0.16 mmol), following the same procedure described for compound **21a**. ¹HNMR (400 MHz, CDCl₃) δ : 9.50 (br s, 2H), 8.18 (d, 2H, $J = 2.0$ Hz), 7.79 (dd, 2H, $J = 2.4$ Hz, $J = 8.8$ Hz), 7.44 (d, 4H, $J = 8.8$ Hz), 7.22 (d, 4H, $J = 8.4$ Hz), 6.97-7.01 (m, 6H), 6.73-6.80 (m, 6H), 6.29 (br s, 2H), 4.49 (t, 4H, $J = 4.8$ Hz), 3.85 (t, 4H, $J = 4.8$ Hz), 3.56-3.72 (m, 44H), 3.51 (t, 4H, $J = 5.0$ Hz), 3.42 (t, 4H, $J = 5.2$ Hz), 3.27 (s, 6H), 3.17 (s, 4H), 2.84 (t, 4H, $J = 7.8$ Hz), 2.67 (s, 4H), 2.42 (t, 4H, $J = 7.8$ Hz), 1.47 (s, 36H); HRMS calcd. for C₁₀₀H₁₄₇N₈O₂₆ (M + H)⁺: 1876.0427, found 1876.0447.

(E)-3-(3-(((2-(tert-Butoxy)-2-oxoethyl)(2-((2-(tert-butoxy)-2-oxoethyl)(5-(1-((5-(4-((tert-butoxycarbonyl)(methyl)amino)styryl)pyridin-2-yl)oxy)-13-oxo-3,6,9-

Imaging A β Plaques in Cerebral Amyloid Angiopathy

1
2
3 **trioxa-12-azapentadecan-15-yl)-2-hydroxybenzyl)amino)ethyl)amino)methyl)-4-**
4
5 **hydroxyphenyl)propanoic acid (22).** Compound **22** (yield: 33 mg, 28.9%): was
6 prepared from **13** (90.4 mg, 0.14 mmol), DIPEA (72.2 mg, 0.56 mmol), HOBt (35.4 mg,
7 0.21 mmol), EDC (40.1 mg, 0.21 mmol), and **20b** (70 mg, 0.14 mmol), following the
8 same procedure described for compound **21a**. ¹HNMR (400 MHz, CDCl₃) δ : 8.17 (d, 1H,
9 $J = 2.0$ Hz), 7.77 (dd, 1H, $J = 2.4$ Hz, $J = 8.8$ Hz), 7.44 (d, 2H, $J = 8.8$ Hz), 7.22 (d, 2H, J
10 = 8.4 Hz), 6.96-7.03 (m, 4H), 6.71-6.78 (m, 5H), 6.55 (br s, 1H), 4.47 (t, 2H, $J = 4.8$ Hz),
11 3.84 (t, 2H, $J = 4.8$ Hz), 3.50-3.72 (m, 16H), 3.40-3.42 (m, 2H), 3.27 (s, 3H), 3.24 (s,
12 4H), 2.82 (t, 4H, $J = 7.4$ Hz), 2.70 (s, 4H), 2.59 (t, 2H, $J = 7.4$ Hz), 2.44 (t, 2H, $J = 7.8$
13 Hz), 1.46 (s, 27H); HRMS calcd. for C₆₁H₈₆N₅O₁₅ (M + H)⁺: 1128.6120, found
14 1128.6105.
15
16
17
18
19
20
21
22
23
24
25
26
27
28
29

30 **2,2'-((E)-Ethane-1,2-diylbis((2-hydroxy-5-(3-((2-(2-(2-((5-((E)-4-**
31 (methylamino)styryl)pyridin-2-yl)oxy)ethoxy)ethoxy)ethyl)amino)-3-
32 **oxopropyl)benzyl)azanediyl))diacetic acid (7a).** A solution of **21a** (30 mg, 0.020
33 mmol) in 1 mL TFA was stirred at rt for 4 h. The reaction mixture was evaporated in
34 vacuo, and the residue was purified by semi-preparative HPLC to give 8.6 mg of a
35 yellow-colored solid, **7a** (yield: 37.6%). ¹HNMR (400 MHz, MeOD) δ : 8.24 (d, 2H, $J =$
36 2.0Hz), 8.02 (dd, 2H, $J = 2.4$ Hz, $J = 8.8$ Hz), 7.70 (d, 4H, $J = 8.4$ Hz), 7.40 (4H, $J = 8.4$
37 Hz), 7.07-7.18 (m, 8H), 6.87 (d, 2H, $J = 8.8$ Hz), 6.80 (d, 2H, $J = 8.8$ Hz), 4.46 (t, 4H, $J =$
38 4.8Hz), 4.10 (s, 4H), 3.85 (t, 4H, $J = 4.6$ Hz), 3.57-3.72 (m, 12H), 3.47 (t, 4H, $J = 5.4$ Hz),
39 3.30-3.32 (m, 8H), 3.06 (s, 6H), 2.80 (t, 4H, $J = 7.4$ Hz), 2.43 (t, 4H, $J = 7.4$ Hz); HRMS
40 calcd. for C₆₆H₈₃N₈O₁₄ (M + H)⁺: 1211.6029, found 1211.6028.
41
42
43
44
45
46
47
48
49
50
51
52
53
54
55
56
57
58
59
60

Imaging A β Plaques in Cerebral Amyloid Angiopathy

1
2
3
4
5
6
7
8
9
10
11
12
13
14
15
16
17
18
19
20
21
22
23
24
25
26
27
28
29
30
31
32
33
34
35
36
37
38
39
40
41
42
43
44
45
46
47
48
49
50
51
52
53
54
55
56
57
58
59
60

2,2'-((*E*)-Ethane-1,2-diylbis((2-hydroxy-5-(1-((5-((*E*)-4-(methylamino)styryl)pyridin-2-yl)oxy)-13-oxo-3,6,9-trioxa-12-azapentadecan-15-yl)benzyl)azanediyl))diacetic acid (7b). Compound **7b** (yield: 8.4 mg, 34.0%): was prepared from **21b** (31 mg, 0.019 mmol) and 1 mL TFA, following the same procedure described for compound **7a**. ¹HNMR(400 MHz, D₂O) δ : 8.43(d, 2H, $J = 9.2$ Hz), 8.24(s, 2H), 7.71(d, 4H, $J = 8.4$ Hz), 7.51(d, 4H, $J = 8.4$ Hz), 7.35(d, 2H, $J = 8.8$ Hz), 7.05-7.21(m, 8H), 6.81(d, 2H, $J = 8.0$ Hz), 4.55(t, 4H, $J = 4.0$ Hz), 4.21(s, 4H), 3.97(t, 4H, $J = 4.0$ Hz), 3.71-3.80(m, 12H), 3.56-3.66(m, 8H), 3.50(s, 4H), 3.46(t, 4H, $J = 5.4$ Hz), 3.26(t, 4H, $J = 5.2$ Hz), 3.13(s, 6H), 2.77(t, 4H, $J = 7.4$ Hz), 2.44(t, 4H, $J = 7.4$ Hz); HRMS calcd for C₇₀H₉₁N₈O₁₆ (M + H)⁺: 1299.6553, found 1299.6506.

28
29
30
31
32
33
34
35
36
37
38
39
40
41
42
43
44
45
46
47
48
49
50
51
52
53
54
55
56
57
58
59
60

2,2'-((*E*)-Ethane-1,2-diylbis((2-hydroxy-5-(1-((5-((*E*)-4-(methylamino)styryl)pyridin-2-yl)oxy)-16-oxo-3,6,9,12-tetraoxa-15-azaoctadecan-18-yl)benzyl)azanediyl))diacetic acid (7c). Compound **7c** (yield: 9.0 mg, 28.2%): was prepared from **21c** (40 mg, 0.023 mmol) and 1 mL TFA following the same procedure described for compound **7a**. ¹HNMR (400 MHz, MeOD) δ : 8.26 (d, 2H, $J = 2.0$ Hz), 8.07 (dd, 2H, $J = 2.4$ Hz, $J = 8.8$ Hz), 7.71 (d, 4H, $J = 8.4$ Hz), 7.43 (d, 4H, $J = 8.4$ Hz), 7.08-7.20 (m, 8H), 6.92 (d, 2H, $J = 8.8$ Hz), 6.81 (d, 2H, $J = 8.8$ Hz), 4.45 (t, 4H, $J = 4.8$ Hz), 4.13 (s, 4H), 3.84 (t, 4H, $J = 4.8$ Hz), 3.53-3.70 (m, 28H), 3.45 (t, 4H, $J = 5.4$ Hz), 3.29-3.35 (m, 8H), 3.07 (s, 6H), 2.81 (t, 4H, $J = 7.4$ Hz), 2.44 (t, 4H, $J = 7.4$ Hz); HRMS calcd. for C₇₄H₉₉N₈O₁₈ (M + H)⁺: 1387.7077, found 1387.7093.

53
54
55
56
57
58
59
60

2,2'-((*E*)-Ethane-1,2-diylbis((2-hydroxy-5-(1-((5-((*E*)-4-(methylamino)styryl)pyridin-2-yl)oxy)-19-oxo-3,6,9,12,15-pentaoxa-18-

Imaging A β Plaques in Cerebral Amyloid Angiopathy

1
2
3 **azahenicosan-21-yl)benzyl)azanediy))diacetic acid (7d).** Compound **7d** (yield: 22 mg,
4 43.8%) was prepared from **21d** (60 mg, 0.034 mmol) and 1 mL TFA, following the same
5 procedure described for compound **7a**. ¹HNMR (400 MHz, MeOD) δ : 7.96 (d, 2H, J =
6 2.0Hz), 7.82 (dd, 2H, J = 2.4Hz, J = 8.8Hz), 7.39 (d, 4H, J = 8.4Hz), 7.14 (d, 4H, J =
7 8.4Hz), 6.77-6.88 (m, 8H), 6.67 (d, 2H, J = 8.8 Hz), 6.50 (d, 2H, J = 8.8 Hz), 4.15 (t, 4H,
8 J = 4.6 Hz), 3.87 (s, 4H), 3.53 (t, 4H, J = 4.4 Hz), 3.44 (s, 4H), 3.20-3.36 (m, 32H), 3.09-
9 3.14 (m, 8H), 2.98 (t, 4H, J = 5.4 Hz), 2.76 (s, 6H), 2.49 (t, 4H, J = 7.4 Hz), 2.13 (t, 4H, J
10 = 7.4 Hz); HRMS calcd. for C₇₈H₁₀₄N₈O₂₀ (M + H)⁺: 1475.7602, found 1475.7187.
11
12
13
14
15
16
17
18
19
20
21
22

23 **2,2'-((E)-Ethane-1,2-diylbis((2-hydroxy-5-(1-((5-((E)-4-**
24 **(methylamino)styryl)pyridin-2-yl)oxy)-22-oxo-3,6,9,12,15,18-hexaoxa-21-**
25 **azatetracosan-24-yl)benzyl)azanediy))diacetic acid (7e).** Compound **7e** (yield: 18.9
26 mg, 37.8%) was prepared from **21e** (60 mg, 0.032 mmol) and 1 mL TFA following the
27 same procedure described for compound **7a**. ¹HNMR (400 MHz, MeOD) δ : 8.28 (d, 2H,
28 J = 2.0Hz), 8.11 (dd, 2H, J = 2.4Hz, J = 8.8Hz), 7.72 (d, 4H, J = 8.4Hz), 7.46 (d, 4H, J =
29 8.4Hz), 7.11-7.25 (m, 8H), 6.96 (d, 2H, J = 8.8 Hz), 6.82 (d, 2H, J = 8.8 Hz), 4.47 (t, 4H,
30 J = 4.8 Hz), 4.16 (s, 4H), 3.86 (t, 4H, J = 4.8 Hz), 3.55-3.73 (m, 44H), 3.45 (t, 4H, J = 5.4
31 Hz), 3.31-3.37 (m, 8H), 3.08 (s, 6H), 2.82 (t, 4H, J = 7.4 Hz), 2.45 (t, 4H, J = 7.4 Hz);
32 HRMS calcd. for C₈₂H₁₁₅N₈O₂₂ (M + H)⁺: 1563.8126, found 1563.8157.
33
34
35
36
37
38
39
40
41
42
43
44
45
46
47

48 **(E)-3-(3-(((Carboxymethyl)(2-((carboxymethyl)(2-hydroxy-5-(1-((5-(4-**
49 **(methylamino)styryl)pyridin-2-yl)oxy)-13-oxo-3,6,9-trioxa-12-azapentadecan-15-**
50 **yl)benzyl)amino)ethyl)amino)methyl)-4-hydroxyphenyl)propanoic acid (8).**
51
52
53
54
55
56
57
58
59
60
Compound **8** (yield: 9.5 mg, 37.1%) was prepared from **22** (31 mg, 0.028 mmol) and 1

Imaging A β Plaques in Cerebral Amyloid Angiopathy

1
2
3 mL TFA, following the same procedure described for compound **7a**. ¹HNMR (400 MHz,
4 MeOD) δ : 8.26 (d, 1H, $J = 2.0$ Hz), 8.11 (dd, 1H, $J = 2.4$ Hz, $J = 8.8$ Hz), 7.72 (d, 2H, $J =$
5 8.4 Hz), 7.40 (d, 2H, $J = 8.4$ Hz), 7.10-7.21 (m, 6H), 6.80-6.91 (m, 3H), 4.47 (t, 2H, $J =$
6 4.4 Hz), 4.16 (s, 2H), 4.11 (s, 2H), 3.86 (t, 2H, $J = 4.4$ Hz), 3.56-3.71 (m, 14H), 3.48 (t,
7 2H, $J = 5.0$ Hz), 3.37 (s, 4H), 3.08 (s, 3H), 2.83 (t, 4H, $J = 7.4$ Hz), 2.56 (t, 2H, $J = 7.6$ Hz),
8 2.46 (t, 2H, $J = 7.4$ Hz); HRMS calcd. for C₄₈H₆₂N₅O₁₃ (M + H)⁺: 916.4344, found
9 916.4436.
10
11
12
13
14
15
16
17
18
19

20
21 [^{nat}Ga]**7a**. A solution of GaCl₃ (1.13 M) in 8 μ L 0.1 N HCl was added to the
22 compound **7a** (10 mg, 7.7 μ mol) in 1 mL H₂O. The mixture was stirred at rt for 1 h. The
23 final complex was determined using LC-MS. HRMS calcd. for C₆₆H₈₀GaN₈O₁₄ (M + H)⁺:
24 1277.5050, found 1277.5081. The resulting aqueous solution of the ^{nat}Ga complex was
25 further diluted and used in the *in vitro* binding affinity study without further processing.
26
27
28
29
30
31
32
33

34 [^{nat}Ga]**7b**. Compound [^{nat}Ga]**7b** was prepared from GaCl₃ (1.13 M) in 9 μ L 0.1 N
35 HCl and **7b** (11 mg, 8.1 μ mol) following the same procedure described for compound
36 [^{nat}Ga]**7a**. HRMS calcd. for C₇₀H₈₈GaN₈O₁₆ (M + H)⁺: 1365.5574, found 1365.5779.
37
38
39
40
41

42 [^{nat}Ga]**7c**. Compound [^{nat}Ga]**7c** was prepared from GaCl₃ (1.13 M) in 8 μ L 0.1 N
43 HCl and **7c** (10 mg, 7.2 μ mol) following the same procedure described for compound
44 [^{nat}Ga]**7a**. HRMS. calcd for C₇₄H₉₆GaN₈O₁₈ (M + H)⁺: 1453.6098, found 1453.6178.
45
46
47
48
49

50 [^{nat}Ga]**7d**. Compound [^{nat}Ga]**7b** was prepared from GaCl₃ (1.13 M) in 7 μ L 0.1 N
51 HCl and **7d** (10 mg, 6.8 μ mol) following the same procedure described for compound
52 [^{nat}Ga]**7a**. HRMS calcd. for C₇₈H₁₀₄GaN₈O₂₀ (M + H)⁺: 1541.6623, found 1541.6689.
53
54
55
56
57
58
59
60

Imaging A β Plaques in Cerebral Amyloid Angiopathy

1
2
3
4
5
6
7
8
9
10
11
12
13
14
15
16
17
18
19
20
21
22
23
24
25
26
27
28
29
30
31
32
33
34
35
36
37
38
39
40
41
42
43
44
45
46
47
48
49
50
51
52
53
54
55
56
57
58
59
60

[^{nat}Ga]7e. Compound [^{nat}Ga]7e was prepared from GaCl₃ (1.13 M) in 7 μ L 0.1 N HCl and 7e (10 mg, 6.4 μ mol) following the same procedure described for compound [^{nat}Ga]7a. HRMS calcd. for C₈₂H₁₁₂GaN₈O₂₂ (M + H)⁺: 1629.7147, found 1629.7166.

[^{nat}Ga]8. Compound [^{nat}Ga]8 was prepared from GaCl₃ (1.13 M) in 8 μ L 0.1 N HCl and 8 (7 mg, 7.6 μ mol) following the same procedure described for compound [^{nat}Ga]7a. HRMS calcd. for C₄₈H₅₉GaN₅O₁₃ (M + H)⁺: 982.3365, found 982.3417.

Radiosynthesis of [⁶⁸Ga] 7a-e and [⁶⁸Ga]8, and stability test. Gallium-68 was obtained from a ⁶⁸Ge/⁶⁸Ga generator (iTG, Germany). A stock solution of ligand (7a-e and 8, 1 mg in 1 mL 0.1 N NaOAc) was prepared and used for the radiolabelling studies. ⁶⁸Ga labeling was performed in aq. NaOAc buffer (15 μ L, 2.0 N) by combining the ligand solution (13 μ L) and ⁶⁸Ga solution (500 μ L in 0.05 N HCl, 2.5-3.1 mCi). The final pH of the mixture was 4.10. Radiolabeling yields were 93-98% after maintaining at rt for 5 min. Radiochemical yields were determined by two TLC systems: A: ITLC-SG (Agilent) developed with 0.1 N citric acid; B: ITLC-SG plates developed with a solvent mixture (H₂O/EtOH/Pyridine = 4/2/1). The HPLC system was developed using an Agilent EC-C18 column (A: 0.1% TFA in H₂O, B: ACN; 0-6 min 100-0% A), 2 mL/min.

The stability of [⁶⁸Ga]7a-e and [⁶⁸Ga]8 was determined by incubating the preparation in PBS (pH = 7.4, 3 h at rt) and human plasma (3 h at 37 °C). ⁶⁸Ga conjugates and free ⁶⁸Ga levels were determined using radio TLC and HPLC as described above.

In vitro binding studies using A β -aggregates in the AD brain tissue homogenates. [¹²⁵I]IMPY with 2200 Ci/mmol specific activity and more than 98%

Imaging A β Plaques in Cerebral Amyloid Angiopathy

1
2
3 radiochemical purity was prepared as described previously⁽⁴⁰⁾. Frozen AD samples were
4
5 homogenized with a tissue homogenizer in PBS. Tissue homogenates were diluted to 50-
6
7 100 mg/mL and frozen at -80 °C until used for the binding assay. Competitive binding
8
9 assays were performed in 12 × 75 mm borosilicate glass tubes by mixing 100 μ L of AD
10
11 brain homogenates, 100 μ L of [¹²⁵I]IMPY, and 50 μ L of competing compounds (10^{-5} to
12
13 10^{-10} M serially diluted in PBS containing 0.1% bovine serum albumin). Nonspecific
14
15 binding was defined by the presence of AV-45 (5.6 μ M) in the same assay tubes. The
16
17 mixture was incubated at rt for 1 h and the bound and free radioactivity were separated by
18
19 vacuum filtration through filter papers (Whatman), a 24-cell harvester (Brandel), and by
20
21 washing with Tris-HCl buffer 3 times. Radioactivity on filters containing the bound
22
23 [¹²⁵I]IMPY was assayed in a γ -counter (Perkin Elmer). The inhibition constant (K_i)
24
25 values were calculated by fitting the data using a nonlinear regression algorithm.
26
27
28
29
30
31
32

33 ***In vitro autoradiography of AD brain sections.*** Frozen AD brains were cut into
34
35 20 μ m sections. The sections were pre-incubated in 40% ethanol at rt and then incubated
36
37 with the ⁶⁸Ga ligands in 40% ethanol at a concentration of 3 nM for 1 h at rt. For blocking
38
39 experiments, an excess of IMPY (28 μ M) was added to the incubation mixture. The
40
41 sections were then dipped in saturated Li₂CO₃ in 40% ethanol (3 min wash once), washed
42
43 with 40% ethanol (3 min wash once), and rinsed with water for 30 s. After drying, the
44
45 sections were exposed to autoradiography film (Denville Scientific) for 20-28 h. After the
46
47 film was developed, the images were digitized.
48
49
50
51
52

53 ***In vivo biodistribution study in CD-1 mice.*** To test [⁶⁸Ga]7a-e and [⁶⁸Ga]8 as
54
55 PET imaging agents for cerebral amyloid angiopathy, we first tested the biodistribution
56
57
58
59
60

Imaging A β Plaques in Cerebral Amyloid Angiopathy

of this tracer in normal CD-1 mice (20-25 grams). A group of 3 mice were used for each time point of the biodistribution study. After the mice were put under anesthesia with isoflurane (2-3%), 0.15 mL saline solution containing 25 μ Ci of the tracer was injected via the lateral tail vein. The mice were sacrificed at 2 and 60 minutes post-injection by cardiac excision while under isoflurane anesthesia. The organs of interest were removed, weighed, and the radioactivity was counted with a gamma counter (Packard Cobra). The percent dose per gram was calculated by a comparison of the tissue activity counts to counts of the injected dose. The injected dose was measured by 1 mL of the injected dose diluted 100 times.

ASSOCIATED CONTENT**Supporting Information**

Chemical synthesis of **14-20**, LC-MS analysis of [nat Ga]**7a**, HPLC profile of [68 Ga]**7a** and coinjected cold compound [nat Ga]**7a**. This material is available free of charge via the Internet at <http://pubs.acs.org>.

ABBREVIATIONS

CAA, cerebral amyloid angiopathy; A β , beta-amyloid; AD, Alzheimer's disease; BBB, blood-brain barrier; PET, positron emission tomography; ICH, intracerebral hemorrhage; MBs, microbleeds; ADRP, AD-related pathology; Amyvid, [18 F]florbetapir; Neuraceq, [18 F]florbetaben; Vizamyl, [18 F]flutemetamol; PiB, Pittsburgh Compound B; 99m Tc-ham, 99m Tc-hydroxamamide; [125 I]IMPY, [125 I]6-iodo-2-(4'-dimethylamino-)phenyl-imidazo[1,2-a]pyridine; K $_i$, Inhibition constant; HBED-CC, N,N'-bis[2-hydroxy-

Imaging A β Plaques in Cerebral Amyloid Angiopathy

5-(carboxyethyl)benzyl]ethylenediamine-N,N'-diacetic acid; DOTA, 1,4,7,10-tetraazacyclododecane-1,4,7,10-tetraacetic acid; NOTA, 1,4,7-triazacyclononane-triacetic acid; NODAGA, (2,2-(7-(1-carboxy-4-(2-mercaptoethylamino)-4-oxobutyl)-1,4,7-triazonane-1,4-diyl)diacetic acid); AAZTA, 6-amino-6-methylperhydro-1,4-diazepinetetraacetic acid; H₂dedpa, 2-[[6-(carboxy)-pyridin-2-yl]-methylamino]ethane; TFA, trifluoroacetic acid; Et₃N, triethylamine; DIPEA, *N,N*-diisopropylethylamine; HOBt, 1-hydroxybenzotriazole hydrate; EDC, *N*-(3-dimethylaminopropyl)-*N*-ethylcarbodiimide hydrochloride.

REFERENCES

- (1) Nicoll, J. A., Burnett, C., Love, S., Graham, D. I., Dewar, D., Ironside, J. W., Stewart, J., and Vinters, H. V. (1997) High frequency of apolipoprotein E ϵ 2 allele in hemorrhage due to cerebral amyloid angiopathy. *Ann. Neurol.* *41*, 716-721.
- (2) Viswanathan, A., and Greenberg, S. M. (2008) Chapter 38 Intracerebral hemorrhage. *Handbook of Clinical Neurology* *93*, 767-790.
- (3) Revesz, T., Holton, J. L., Lashley, T., Plant, G., Frangione, B., Rostagno, A., and Ghiso, J. (2009) Genetics and molecular pathogenesis of sporadic and hereditary cerebral amyloid angiopathies. *Acta Neuropathol. (Berl.)* *118*, 115-130.
- (4) Brenowitz, W. D., Nelson, P. T., Besser, L. M., Heller, K. B., and Kukull, W. A. (2015) Cerebral amyloid angiopathy and its co-occurrence with Alzheimer's disease and other cerebrovascular neuropathologic changes. *Neurobiol. Aging*.
- (5) Adeoye, O., and Broderick, J. P. (2010) Advances in the management of intracerebral hemorrhage. *Nature Reviews Neurology* *6*, 593-601.
- (6) Rosand, J., and Greenberg, S. M. (2000) CEREBRAL AMYLOID ANGIOPATHY. *The Neurologist* *6*, 315-325.
- (7) Corder, E. H., Saunders, A. M., Strittmatter, W. J., Schmechel, D. E., Gaskell, P. C., Small, G. W., Roses, A. D., Haines, J. L., and Pericak-Vance, M. A. (1993) Gene dose of apolipoprotein E type 4 allele and the risk of Alzheimer's disease in late onset families. *261*, 921-923.

Imaging A β Plaques in Cerebral Amyloid Angiopathy

- 1
2
3
4
5
6
7
8
9
10
11
12
13
14
15
16
17
18
19
20
21
22
23
24
25
26
27
28
29
30
31
32
33
34
35
36
37
38
39
40
41
42
43
44
45
46
47
48
49
50
51
52
53
54
55
56
57
58
59
60
- (8) Ringman, J. M., Sachs, M. C., Zhou, Y., Monsell, S. E., Saver, J. L., and Vinters, H. V. (2014) Clinical predictors of severe cerebral amyloid angiopathy and influence of APOE genotype in persons with pathologically verified Alzheimer disease. *JAMA neurology* 71, 878-883.
- (9) Ellis, R., Olichney, J., Thal, L., Mirra, S., Morris, J., Beekly, D., and Heyman, A. (1996) Cerebral amyloid angiopathy in the brains of patients with Alzheimer's disease The CERAD experience, part XV. *Neurology* 46, 1592-1596.
- (10) Jellinger, K. (2002) Alzheimer disease and cerebrovascular pathology: an update. *J. Neural Transm.* 109, 813-836.
- (11) Thal, D. R., Ghebremedhin, E., Orantes, M., and Wiestler, O. D. (2003) Vascular pathology in Alzheimer disease: correlation of cerebral amyloid angiopathy and arteriosclerosis/lipohyalinosis with cognitive decline. *J. Neuropathol. Exp. Neurol.* 62, 1287-301.
- (12) Wong, D., Rosenberg, P., Zhou, Y., Kumar, A., Raymont, V., Ravert, H., Dannals, R., Nandi, A., Brasic, J., Ye, W., et al. (2010) In Vivo Imaging of Amyloid Deposition in Alzheimer Disease Using the Radioligand 18F-AV-45 (Florbetapir F 18). *J. Nucl. Med.* 51, 913-920.
- (13) Kung, H., Choi, S., Qu, W., Zhang, W., and Skovronsky, D. (2009) (18)F Stilbenes and Styrylpyridines for PET Imaging of Abeta Plaques in Alzheimer's Disease: A Miniperspective. *J. Med. Chem.* 53, 933-941.
- (14) Choi, S., Golding, G., Zhuang, Z., Zhang, W., Lim, N., Hefti, F., Benedum, T., Kilbourn, M., Skovronsky, D., and Kung, H. (2009) Preclinical properties of 18F-AV-45: a PET agent for A β plaques in the brain. *J. Nucl. Med.* 50, 1887-1894.
- (15) Zhang, W., Kung, M., Oya, S., Hou, C., and Kung, H. (2007) (18)F-labeled styrylpyridines as PET agents for amyloid plaque imaging. *Nucl. Med. Biol.* 34, 89-97.
- (16) Clark, C. M., Schneider, J. A., Bedell, B. J., Beach, T. G., Bilker, W. B., Mintun, M. A., Pontecorvo, M. J., Hefti, F., Carpenter, A. P., Flitter, M. L., et al. (2011) Use of florbetapir-PET for imaging beta-amyloid pathology. *JAMA* 305, 275-83.
- (17) O'Keefe, G., Saunder, T., Ng, S., Ackerman, U., Tochon-Danguy, H., Chan, J., Gong, S., Dyrks, T., Lindemann, S., Holl, G., et al. (2009) Radiation Dosimetry of {beta}-Amyloid Tracers 11C-PiB and 18F-BAY94-9172. *J. Nucl. Med.* 50, 309-315.
- (18) Rowe, C., Ackerman, U., Browne, W., Mulligan, R., Pike, K., O'Keefe, G., Tochon-Danguy, H., Chan, G., Berlangieri, S., Jones, G., et al. (2008) Imaging of amyloid beta in Alzheimer's disease with 18F-BAY94-9172, a novel PET tracer: proof of mechanism. *Lancet Neurol.* 7, 129-35.
- (19) Zhang, W., Oya, S., Kung, M., Hou, C., Maier, D., and Kung, H. H. (2005) F-18 Polyethyleneglycol stilbenes as PET imaging agents targeting A β aggregates in the brain. *Nucl. Med. Biol.* 32, 799-809.
- (20) Zhang, W., Oya, S., Kung, M., Hou, C., Maier, D., and Kung, H. (2005) F-18 Stilbenes as PET Imaging Agents for Detecting beta-Amyloid Plaques in the Brain. *J. Med. Chem.* 48, 5980-8.

Imaging A β Plaques in Cerebral Amyloid Angiopathy

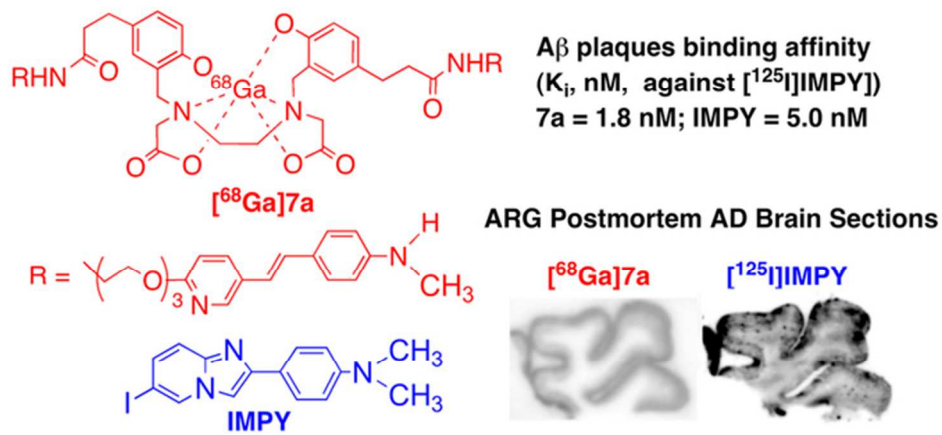
- 1
2
3
4
5
6
7
8
9
10
11
12
13
14
15
16
17
18
19
20
21
22
23
24
25
26
27
28
29
30
31
32
33
34
35
36
37
38
39
40
41
42
43
44
45
46
47
48
49
50
51
52
53
54
55
56
57
58
59
60
- (21) Koole, M., Lewis, D., Buckley, C., Nelissen, N., Vandenbulcke, M., Brooks, D., Vandenberghe, R., and Van Laere, K. (2009) Whole-body biodistribution and radiation dosimetry of 18F-GE067: a radioligand for in vivo brain amyloid imaging. *J. Nucl. Med.* 50, 818-822.
- (22) Nelissen, N., Van Laere, K., Thurfjell, L., Owenius, R., Vandenbulcke, M., Koole, M., Bormans, G., Brooks, D. J., and Vandenberghe, R. (2009) Phase 1 study of the Pittsburgh compound B derivative 18F-flutemetamol in healthy volunteers and patients with probable Alzheimer disease. *J. Nucl. Med.* 50, 1251-9.
- (23) Vandenberghe, R., Van Laere, K., Ivanoiu, A., Salmon, E., Bastin, C., Triau, E., Hasselbalch, S., Law, I., Andersen, A., Korner, A., et al. (2010) 18F-flutemetamol amyloid imaging in Alzheimer disease and mild cognitive impairment: A phase 2 trial. *Ann. Neurol.* 68, 319-329.
- (24) Thomas, B. A., Erlandsson, K., Modat, M., Thurfjell, L., Vandenberghe, R., Ourselin, S., and Hutton, B. F. (2011) The importance of appropriate partial volume correction for PET quantification in Alzheimer's disease. *Eur. J. Nucl. Med. Mol. Imaging* 38, 1104-1119.
- (25) Gurol, M. E., Dierksen, G., Betensky, R., Gidicsin, C., Halpin, A., Becker, A., Carmasin, J., Ayres, A., Schwab, K., and Viswanathan, A. (2012) Predicting sites of new hemorrhage with amyloid imaging in cerebral amyloid angiopathy. *Neurology* 79, 320-326.
- (26) Johnson, K. A., Gregas, M., Becker, J. A., Kinnecom, C., Salat, D. H., Moran, E. K., Smith, E. E., Rosand, J., Rentz, D. M., Klunk, W. E., et al. (2007) Imaging of amyloid burden and distribution in cerebral amyloid angiopathy. *Ann. Neurol.* 62, 229-34.
- (27) Ly, J., Donnan, G., Villemagne, V., Zavala, J., Ma, H., O'Keefe, G., Gong, S., Gunawan, R., Saunder, T., Ackerman, U., et al. (2010) 11C-PIB binding is increased in patients with cerebral amyloid angiopathy-related hemorrhage. *Neurology* 74, 487-493.
- (28) Greenberg, S. M., Grabowski, T., Gurol, M. E., Skehan, M. E., Nandigam, R. N., Becker, J. A., Garcia-Alloza, M., Prada, C., Frosch, M. P., Rosand, J., et al. (2008) Detection of isolated cerebrovascular beta-amyloid with Pittsburgh compound B. *Ann. Neurol.* 64, 587-91.
- (29) Reijmer, Y. D., Fotiadis, P., Martinez-Ramirez, S., Salat, D. H., Schultz, A., Shoamanesh, A., Ayres, A. M., Vashkevich, A., Rosas, D., and Schwab, K. (2014) Structural network alterations and neurological dysfunction in cerebral amyloid angiopathy. *Brain*, awu316.
- (30) Sengoku, R., Matsushima, S., Murakami, Y., Fukuda, T., Tokumaru, A. M., Hashimoto, M., Suzuki, M., Ishiwata, K., Ishii, K., and Mochio, S. (2014) 11 C-PiB PET Imaging of Encephalopathy Associated with Cerebral Amyloid Angiopathy. *Intern. Med.* 53, 1997-2000.
- (31) Lockhart, A., Lamb, J. R., Osredkar, T., Sue, L. I., Joyce, J. N., Ye, L., Libri, V., Leppert, D., and Beach, T. G. (2007) PIB is a non-specific imaging marker of amyloid-beta (A β) peptide-related cerebral amyloidosis. *Brain* 130, 2607-15.

Imaging A β Plaques in Cerebral Amyloid Angiopathy

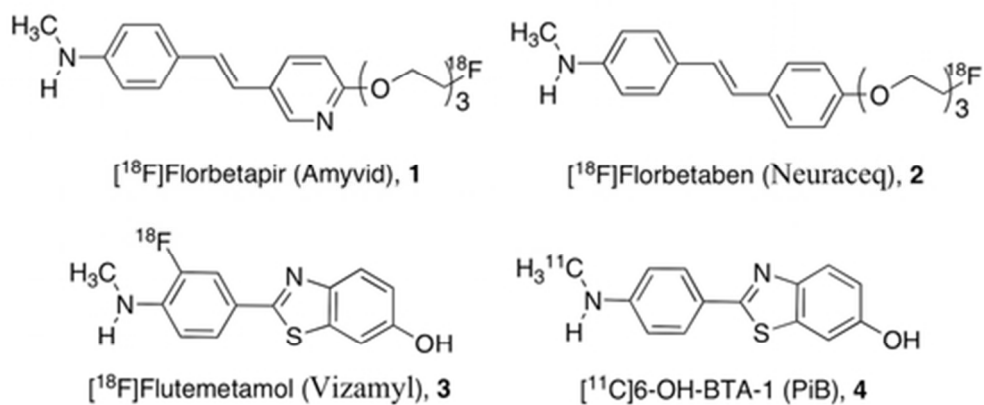
- 1
2
3
4
5
6
7
8
9
10
11
12
13
14
15
16
17
18
19
20
21
22
23
24
25
26
27
28
29
30
31
32
33
34
35
36
37
38
39
40
41
42
43
44
45
46
47
48
49
50
51
52
53
54
55
56
57
58
59
60
- (32) Jia, J., Cui, M., Dai, J., and Liu, B. (2015) 99mTc (CO) 3-Labeled Benzothiazole Derivatives Preferentially Bind Cerebrovascular Amyloid: Potential Use as Imaging Agents for Cerebral Amyloid Angiopathy. *Mol. Pharm.* *12*, 2937-2946.
- (33) Liu, S. (2009) Radiolabeled Cyclic RGD Peptides as Integrin $\alpha(v)\beta(3)$ -Targeted Radiotracers: Maximizing Binding Affinity via Bivalency. *Bioconjugate Chem.* *20*, 2199-2213.
- (34) Capule, C. C., Brown, C., Olsen, J. S., Dewhurst, S., and Yang, J. (2012) Oligovalent amyloid-binding agents reduce SEVI-mediated enhancement of HIV-1 infection. *J. Am. Chem. Soc.* *134*, 905-908.
- (35) Bastings, M. M., Helms, B. A., van Baal, I., Hackeng, T. M., Merckx, M., and Meijer, E. (2011) From phage display to dendrimer display: Insights into multivalent binding. *J. Am. Chem. Soc.* *133*, 6636-6641.
- (36) Deyev, S. M., and Lebedenko, E. N. (2008) Multivalency: the hallmark of antibodies used for optimization of tumor targeting by design. *BioEssays* *30*, 904-918.
- (37) Mammen, M., Choi, S.-K., and Whitesides, G. M. (1998) Polyvalent interactions in biological systems: implications for design and use of multivalent ligands and inhibitors. *Angewandte Chemie International Edition* *37*, 2754-2794.
- (38) Iikuni, S., Ono, M., Watanabe, H., Matsumura, K., Yoshimura, M., Harada, N., Kimura, H., Nakayama, M., and Saji, H. (2014) Enhancement of Binding Affinity for Amyloid Aggregates by Multivalent Interactions of 99mTc-Hydroxamamide Complexes. *Mol. Pharm.* *11*, 1132-1139.
- (39) Zha, Z., Choi, S. R., Ploessl, K., Lieberman, B. P., Qu, W., Hefti, F., Mintun, M., Skovronsky, D., and Kung, H. F. (2011) Multidentate 18F-polypegylated styrylpyridines as imaging agents for Abeta plaques in cerebral amyloid angiopathy (CAA). *J. Med. Chem.* *54*, 8085-98.
- (40) Kung, H. F. (2002) Synthesis and characterization of 125I/123I IMPY as an abeta-plaque imaging agent. *J. Nucl. Med.* *43*, 166P.
- (41) Motekaitis, R. J., Martell, A. E., and Welch, M. J. (1990) Stability of trivalent metal complexes of phenolic acids related to N,N'-bis(2-hydroxybenzyl)-N,N'-diacetic acid (HBED). *Inorg. Chem.* *29*, 1463-1467.
- (42) Haberkorn, U., Eder, M., Kopka, K., Babich, J. W., and Eisenhut, M. (2016) New Strategies in Prostate Cancer: Prostate-Specific Membrane Antigen (PSMA) Ligands for Diagnosis and Therapy. *Clin. Cancer Res.* *22*, 9-15.
- (43) Eder, M., Neels, O., Muller, M., Bauder-Wust, U., Remde, Y., Schafer, M., Hennrich, U., Eisenhut, M., Afshar-Oromieh, A., Haberkorn, U., et al. (2014) Novel Preclinical and Radiopharmaceutical Aspects of [68Ga]Ga-PSMA-HBED-CC: A New PET Tracer for Imaging of Prostate Cancer. *Pharmaceuticals (Basel)* *7*, 779-96.
- (44) Kung, M., Hou, C., Zhuang, Z., Cross, A., Maier, D., and Kung, H. (2004) Characterization of IMPY as a potential imaging agent for β -amyloid plaques in double transgenic PSAPP mice. *Eur. J. Nucl. Med. Mol. Imaging* *31*, 1136-1145.
- (45) Ebenhan, T., Vorster, M., Marjanovic-Painter, B., Wagener, J., Suthiram, J., Modiselle, M., Mokaleng, B., Zeevaart, J. R., and Sathekge, M. (2015)

Imaging A β Plaques in Cerebral Amyloid Angiopathy

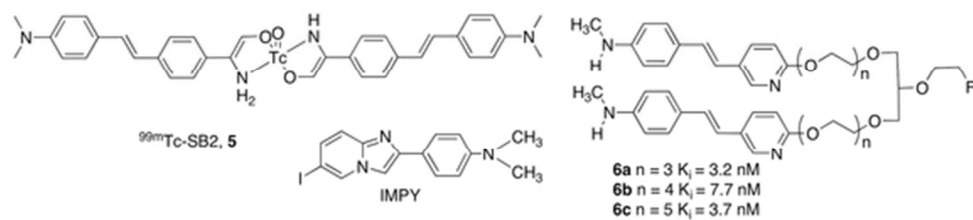
- Development of a Single Vial Kit Solution for Radiolabeling of (68)Ga-DKFZ-PSMA-11 and Its Performance in Prostate Cancer Patients. *Molecules* 20, 14860-78.
- (46) Price, E. W., and Orvig, C. (2014) Matching chelators to radiometals for radiopharmaceuticals. *Chem. Soc. Rev.* 43, 260-90.
- (47) Kubicek, V., Havlickova, J., Kotek, J., Tircso, G., Hermann, P., Toth, E., and Lukes, I. (2010) Gallium(III) complexes of DOTA and DOTA-monoamide: kinetic and thermodynamic studies. *Inorg. Chem.* 49, 10960-9.
- (48) Stasiuk, G. J., and Long, N. J. (2013) The ubiquitous DOTA and its derivatives: the impact of 1,4,7,10-tetraazacyclododecane-1,4,7,10-tetraacetic acid on biomedical imaging. *Chem. Commun. (Camb.)* 49, 2732-46.
- (49) Morfin, J.-F., and Toth, E. (2011) Kinetics of Ga(NOTA) Formation from Weak Ga-Citrate Complexes. *Inorg. Chem.* 50, 10371-10378.
- (50) Sun, Y., Anderson, C. J., Pajeau, T. S., Reichert, D. E., Hancock, R. D., Motekaitis, R. J., Martell, A. E., and Welch, M. J. (1996) Indium (III) and gallium (III) complexes of bis(aminoethanethiol) ligands with different denticities: stabilities, molecular modeling, and in vivo behavior. *J. Med. Chem.* 39, 458-70.
- (51) Eisenwiener, K. P., Prata, M. I., Buschmann, I., Zhang, H. W., Santos, A. C., Wenger, S., Reubi, J. C., and Macke, H. R. (2002) NODAGATOC, a new chelator-coupled somatostatin analogue labeled with [67/68Ga] and [111In] for SPECT, PET, and targeted therapeutic applications of somatostatin receptor (hsst2) expressing tumors. *Bioconjug. Chem.* 13, 530-41.
- (52) Eder, M., Krivoshein, A. V., Backer, M., Backer, J. M., Haberkorn, U., and Eisenhut, M. (2010) ScVEGF-PEG-HBED-CC and scVEGF-PEG-NOTA conjugates: comparison of easy-to-label recombinant proteins for [68Ga]PET imaging of VEGF receptors in angiogenic vasculature. *Nucl. Med. Biol.* 37, 405-12.
- (53) Eder, M., Wangler, B., Knackmuss, S., LeGall, F., Little, M., Haberkorn, U., Mier, W., and Eisenhut, M. (2008) Tetrafluorophenolate of HBED-CC: a versatile conjugation agent for 68Ga-labeled small recombinant antibodies. *Eur. J. Nucl. Med. Mol. Imaging* 35, 1878-86.
- (54) Baranyai, Z., Uggeri, F., Maiocchi, A., Giovenzana, G. B., Cavallotti, C., Takacs, A., Toth, I., Banyai, I., Benyei, A., Brucher, E., et al. (2013) Equilibrium, Kinetic and Structural Studies of AAZTA Complexes with Ga³⁺, In³⁺ and Cu²⁺. *Eur. J. Inorg. Chem.* 2013, 147-162.
- (55) Waldron, B. P., Parker, D., Burchardt, C., Yufit, D. S., Zimny, M., and Roesch, F. (2013) Structure and stability of hexadentate complexes of ligands based on AAZTA for efficient PET labelling with gallium-68. *Chem. Commun. (Camb.)* 49, 579-81.



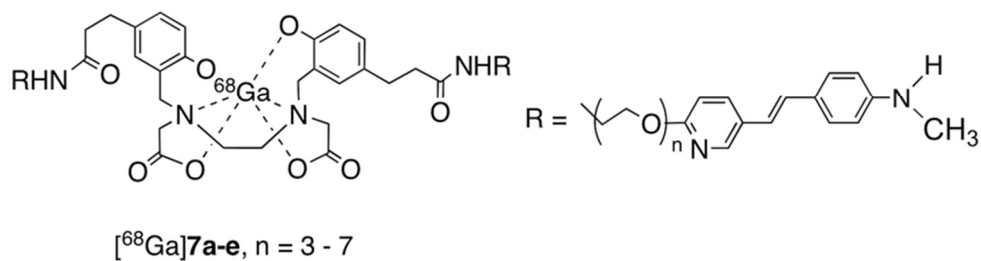
Graphical Abstract
61x27mm (300 x 300 DPI)



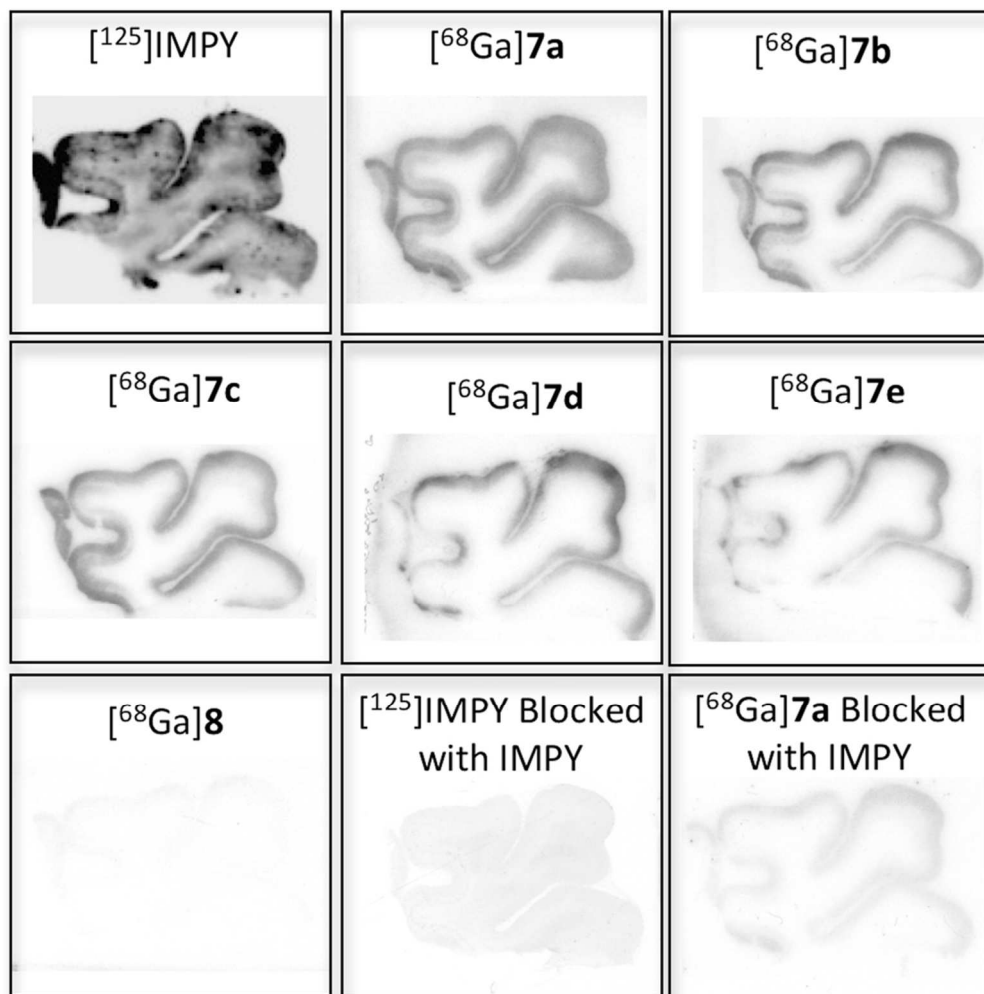
Chemical structures of various PET ligands targeting A β plaques in the brain.
44x19mm (300 x 300 DPI)



Chemical structures of bivalent ligands and IMPY-targeting A β plaques in the brain. All of the compounds have been previously reported. ⁽³⁸⁻⁴⁰⁾
50x11mm (300 x 300 DPI)

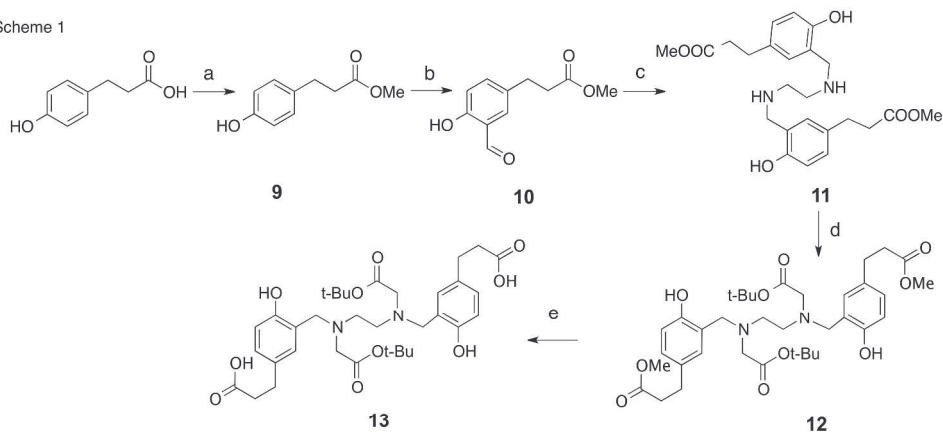


17 Structure of bivalent ligands $[^{68}\text{Ga}]\mathbf{7a-e}$, based on styrylpyridine cores. The novel compounds are designed
18 to bind to $\text{A}\beta$ aggregates via multiple binding sites.
19 73x20mm (300 x 300 DPI)
20
21
22
23
24
25
26
27
28
29
30
31
32
33
34
35
36
37
38
39
40
41
42
43
44
45
46
47
48
49
50
51
52
53
54
55
56
57
58
59
60



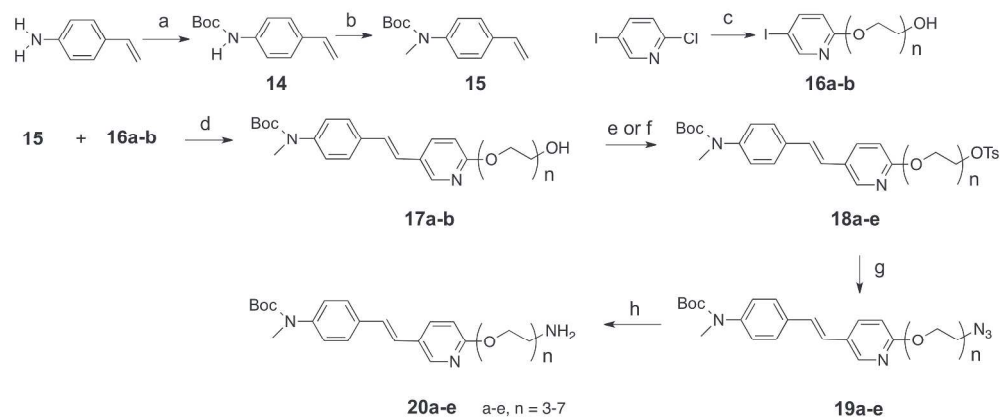
41 In vitro autoradiography of brain sections from AD patients labeled with [¹²⁵I]IMPY, [⁶⁸Ga]7a-e, and
42 [⁶⁸Ga]8. [¹²⁵I]IMPY and [⁶⁸Ga]7a binding in AD brain sections blocked in the presence of 28 μM IMPY.
43 89x90mm (300 x 300 DPI)

Scheme 1



Reagent and conditions: (a) MeOH, $\text{BF}_3 \cdot \text{Et}_2\text{O}$, rt; (b) $(\text{CHO})_n$, MgCl_2 , Et_3N , ACN, reflux; (c) ethylenediamine, NaBH_4 , MeOH, 50 °C, rt; (d) tert-Butyl bromoacetate, Na_2CO_3 , ACN, 60 °C; (e) NaOH, MeOH, H_2O , rt.

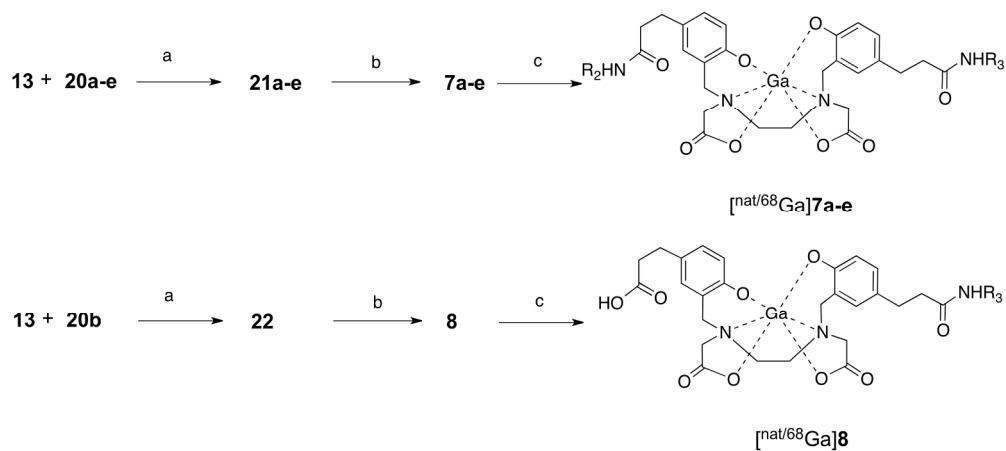
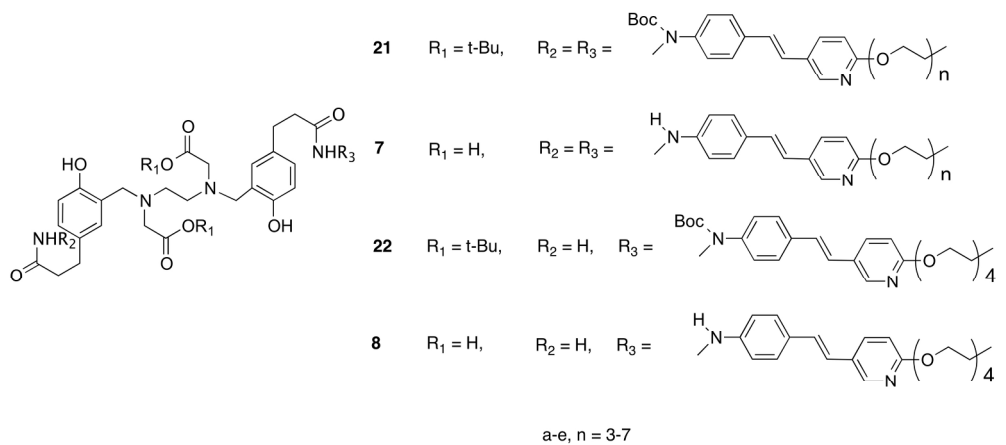
Scheme 2



Reagent and conditions: (a) $(\text{Boc})_2\text{O}$, H_2O , 35 °C; (b) NaH, CH_3I , DMF, rt; (c) triethylene glycol or tetraethylene glycol, Cs_2CO_3 , DMF, 150 °C; (d) K_2CO_3 , Bu_4NBr , $\text{Pd}(\text{OAc})_2$, DMF, 60 °C; (e) TsCl, Et_3N , DMAP, DCM, rt; (f) diethylene glycol ditosylate or triethylene glycol ditosylate, NaH, DMF, rt; (g) NaN_3 , DMF, 60 °C; (h) PPh_3 , H_2O , THF, 68 °C.

242x271mm (600 x 600 DPI)

Scheme 3



Reagent and conditions: (a) EDCI, HOBT, DIPEA, DMF, rt; (b) TFA, rt; (c) [^{nat/68}Ga]GaCl₃, H₂O, rt.

208x212mm (300 x 300 DPI)